PEOPULE'S DEMOCRATIC REPUBLIC OF ALGERIA

Ministry of Higher Education and Scientific Research

N° d'ordre :
N° de série :

University of Echahid Hamma Lakhdar – El-Oued

Institute of Exact Sciences

A Dissertation Submitted to the Department of Physics

In Partial Fulfillment of the Requirements

For the Degree of Master in

Applied Physics: Radiation and Energy

by**: Nadjet GHERAISSA**

Title

Numerical Study of Bio Fuels Combustion

Members of jury:

Dr. Samia DILMI	MCB	University of Echahid Hamma LakhdarEl-Oued	President
Dr. Fethi BOURAS	MCA	University of Echahid Hamma LakhdarEl-Oued	Supervisor
Dr. Fathi LETAIM	MAA	University of Echahid Hamma LakhdarEl-Oued	Examiner

EL OUED: 25/05/2016

Acknowledgements

First of all I would like to thank God, the almighty for providing me this opportunity and granting me the capability to finishing this master thesis.

I would like to convey my sincere gratitude to my thesis supervisor Dr. Fethi BOURAS for the guidance, encouragement throughout the development of this work.

I would especially like to thank the members of the reading committee Dr. Samia DILMI & Dr. Fathi LETAIM for their acceptance to examine my thesis.

I also wish to thank Mr.M.E.ATTIA & my uncle Slimane for helping me.

I convey my sincere thanks to my friends:
Rabab, Fatima, Amel, Laila.

Last but never least, I want to express my deep thanks to my dear parents for encouragement and support throughout my life.

Nadjet

To My Father & My Mother

... To All My Family

Table of Contents

List of Figures

Nomenclature

Latin letters:

A	Deformation tensor
C	Specific heat
c	Parameter progress
C_s	Smagorinsky coefficient
C_w	Constant WALE
D	Diameter
E	Energy
e	Internal energy
F	Field describes the rate of the conserved variables.
h_i	Enthalpy of species i
$\tilde{g}_{ij}^2$	Velocity gradient resolved
k	kinetic energy
L	Large-scale Kolmogorov flow
N	Number of chemical species
n	Boundary-normal coordinate
n_i	The number of moles of the species i
p	Pressure
P( )	Probability density function
F( )	the probability function.
Pr	Prandtl number
q_R	Radiative heat flux vector
Q	Conserved variables.
R	ideal gas constant
Re	Reynolds number
s	Source Term
$\tilde{S}_{ij}$	Tensor velocity deformation

t	Time
T	Temperature
u	Velocity
u_α	Velocity component
V_i	Mass diffusion velocity of species i
x_i	The mole fraction of species i
y	The distance to the normalized wall
y_i	Mass fraction of species i
Z	Mixture fraction

Greek Symbol:

ρ	Mass density
λ	Thermal conductivity
κ	Thermal diffusivity
σ	Stress tensor
μ	Dynamic viscosity
ν	kinematic viscosity
μ_T	Turbulent viscosity
η	Small-scale Kolmogorov flow
ω_i	Chemical production rate of species i
τ_{ij}	Viscous stress tensor
$\Gamma( )$	Gamma function
δ_{ij}	Kronecker delta

Index:

f	*Chemical Species*
i	*Components along the axes x, y and z*
r	*Radial coordinate*
x	*Spatial coordinate*

Abbreviations:

CFD	Computational Fluid Dynamics
CRZ	Central Recirculation Zone
DNS	Direct Numerical Simulation
FPDF	Filtered Probability Density Function
GUI	graphical user interface
LES	Large eddy simulation
PDF	Probability Density Function
RANS	Reynolds Averaged Navier Stokes
SGS	Sub-grid scale
WALE	Wall Adapting Local Eddy Viscosity

General Introduction

General Introduction

The conversion of Biomass into useful energy is done through various types of processes. The choice of the type of conversion process depends on the type, quantity, raw material properties, but also by the end user, the latter being able to put constraints of cost, environmental, or related to a specific design project. Biomass has always been a reliable source of energy, from the first man-made fire up to the utilization of pelletized wood as a feed for thermal plants. Although the use of lignocellulosic feedstock as a solid Bio fuel is a well-known concept, conversion of mass into liquid fuel is a considerable challenge, and the more complex the Biomass gets (in terms of chemical composition) the more complicated and generally expensive the conversion process becomes [1]. The concurring phenomena of world energy need increasing and oil stocks decreasing have generated an increased interest toward Bio fuels in the last 10 to 20 years, although for most of the 20th century, research on Bio fuel closely depended on the price trend of petroleum. Bio fuels can be defined are fuels produced from biological material, a definition that can also be applied to renewable sources of carbon. Use of ethanol for lamp oil and cooking has been reported for decades (called spirit oil at the time) before Samuel Morey first tested it in an internal combustion engine in early 19th century. Ethanol then replaced whale oil before being replaced by petroleum distillate (starting with kerosene for lighting). By the end of the 19th century, ethanol was used in farm machinery and introduced in the automobile market. Oil-derived products replaced ethanol for most of the 20th century before being introduced again during the Arab oil embargo in the 1970s when the price of petroleum and its derivatives peaked [2].

Li Zhou et al (2015) are investigated in the experimental analysis of the excess molar enthalpy data of the ternary systems and the corresponding binary systems at T = 298.15 and 313.15 K at atmospheric pressure [3]. The experimental data are fitted using the Redlich–Kister rational polynomials. Where the binary systems mixtures are shown endothermic effect and strong asymmetric behavior at the measured temperatures [4]. In 2015, G. Gonca is studied the influences of steam injection on the adiabatic flame temperatures, and is verified the simulation code with experimental studies to determine and to compare the combustion characteristics of Bio fuels and conventional diesel fuel. The results show that that the alcohols combustion produce minimum NO emissions. And the injection of Bio fuels as a diesel engine fuel could be decrease pollutants [5]. Dimitrios *et al* (2014) are present experimental study to evaluate the effects of the blends of diesel fuel with different compositions in the combustion performance and exhaust emissions. Fuel injection and cylinder pressure diagrams. The results of

experimental heat release analysis of the acquired fuel injection pressure and the different physical and chemical properties of the Bio fuels flame behavior in the engine [6]. Cameretti *et al* (2013) are discussed some aspects related to employment the liquid and gaseous Bio fuels in a typical lean premixed combustor of a micro-gas turbine. In addition, the purpose checking is the effectiveness methods for supplying the micro-turbine with fuels from renewable sources. For the liquid fuel is modified position of the pilot injector to find the optimal combination of the injector location to minimizing the emissions in a wide range of the micro gas turbine operation supplied by both natural gas and gaseous Bio fuels[7]. Brynolf *et al* (2014) are compared the methane, Bio fuels, methanol and the natural gas as a fuels and their impact on the environment and their energy performance as raw materials. For this raison a transition to use of LNG (Life cycle assessment) is used to produce the methanol from natural gas to improve the overall environmental performance [8]. G.I. Pearman (2013) is examined the bio-physical limits of Bio fuels and bio-sequestration of carbon by solar radiation incident, and he is observed the efficiencies with which natural ecosystems and agricultural systems convert that energy to Biomass. The results demonstrate that the Bio fuels or bio-sequestration can only be a small part of an inclusive portfolio of actions towards a low carbon future and minimize the net emissions of carbon to the atmosphere [9]. Morales *et al*. (2014) are performed an optical and thermal analysis of the Bio fuel process using solar pyrolysis of orange peels. The solar radiation is applied as a unique source of energy using a parabolic-trough solar concentrator; and an optical analysis conduct to use a Monte Carlo ray-tracing method to provide the tridimensional description of the optical performance of the thermo-solar system. Also, the need to identify new renewable energy sources allows the demonstration the solid agro-industrial waste management approach. Where, the solar pyrolytic processes could become important methods for producing solar liquids fuels because of their potential for converting unlimited amounts of solar energy into chemical energy [10]. Han et al (2013) are studied the analysis of bio-based aviation fuels and compared it with petroleum fuel. A sensitivity analysis of the key parameters of fuel production is conducted to identify the most important factors impacting of the pollutants emission, showing the importance of Biomass fuels share in the overall efficiency [11]. Aguilar *et al* (2013) illustrate a new experimental study based on the molar enthalpy analysis at atmospheric pressure. Where this study is based on the ternary systems dibutyl ether (DBE) and butanol and 1-hexene at 298.15 K and 313.15 K. And, butanol and cyclohexane trimethylpentane (TMP) at 313.15 K. Whereof, the isothermal excess molar enthalpies is determined by using a quasi-isothermal flow calorimeter. The results show that the ternary systems show that the addition of the hexene decreases the endothermic effect of the ether-alkanol mixture [12]. Bouras

et al (2013) are investigated the entropy generation rate in the turbulent non-premixed combustion of methane/air in the coaxial jets. Where, this work is based on the validation of this study with experimental referenced data .ie, of axial velocity, temperature and mass fraction of carbon monoxide (CO). The numerical calculations are carried out by FLUENT-CFD including an integrated entropy generation function in C++ language using UDMs. The results prove that the chemical reaction and the heat transfer entropy generation sources are more important responsible of thermodynamic irreversibilities while the viscous friction irreversibility is negligible [13].

This work addressed the numerical study of non-premixed combustion in a three-dimensional cylindrical chamber fueled by Biofuel/air. The present study focused on find thermo-chemical dynamic characteristics of the combustion reaction. Whereas, the system is handled by using the LES & PDF models. Where modeling and calculation are carried out by the software package FLUENT-CFD.

The parts of the thesis have been organized as below:

Chapter I:

Initially, we present mathematical models for each of the LES & PDF. And, how can be surmount the closure in the equations.

Chapter II:

After that, we give the most important stapes of modeling the non-premixed combustion in a three-dimensional cylindrical combustion chamber by FLUENT_CFD.

Chapter III:

Finally, a numerical results is verified by experimental data, and compared with the kinetic, thermal and chemical properties for specific locations in the combustion chamber.

CHAPTER I

Turbulent Non Premixed Combustion Modeling

CHAPTER I Turbulent Non Premixed Combustion Modeling

The turbulence has an effect which improve the reactive mixture. Whereof, the combustion modeling gives the opportunity in the combustion engines development. The progress in computational material and numerical process allows the accessibility to complex configurations. Nevertheless, the turbulent flow is characterized by the fluctuations; this makes the turbulent flows simulation very difficult. Thereby, the fluctuations are modeled by the method using statistical averaging calculations.

In this chapter, we are going to present a basic theory of turbulence based on the statistical analysis applying to the non-premixed combustion. Moreover, the two models are given in the next, and they are the key of interest of the prediction and the modeling flows: turbulence model of LES and the thermo-chemical model of PDF combustion.

I.1 Turbulent Flow

Turbulence is the chaotic state of fluid motion, which is characterized by apparently random and chaotic three-dimensional vorticity. When turbulence appears in the overall flow and dominate the phenomena including in the flows, and it results the increase in the energy dissipation, mixing and heat transfer. The turbulent flows are characterized by the occurrence of the different lengths and scales eddies. In figure I.1, the turbulent coaxial jets inject the fuel by the center one and the air in the surroundings to the central jet, with difference between both velocity air/ Fuel. This may create by the meeting the shearing layer, where the fuel and air are mixing. That is the rich zone where the flame can seat on, and it is created to improve the reactive mixture [14, 15, 16].

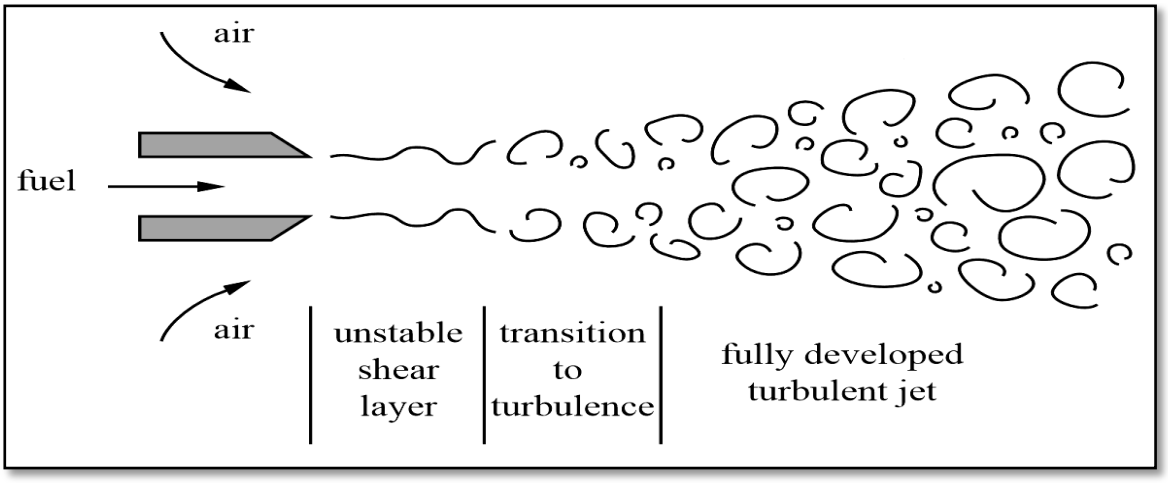

Figure I.1 Schematic presentation of turbulent jet [15].

This morphology of the flow is the aims of many experimental and numerical studies, where the successful modeling of turbulence for large scales are investigated. Turbulence is one of the greatest unsolved problems of classical fluid physics [17].

I.2 Statistical Description of Turbulent Flows

I.2.1 Reynolds Average

Reynolds have considered the average concept in 1895 [16]. This theory is based on decomposing the flow parameter in two components: the average value $\bar{u}$ and fluctuate u' component (figure I.2). Where the Reynolds average is defined by [18]:

$$u = \bar{u} + u' \tag{I.1}$$

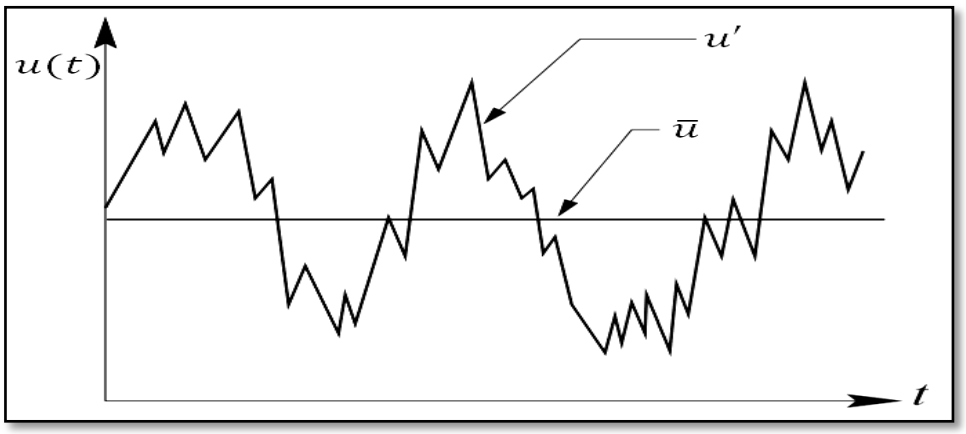

Figure I.2 Illustration of the parameters decomposition in turbulent flow [19].

The Reynolds averaged velocities are:

$$\bar{u} = \lim_{T\to\infty} \frac{1}{T} \int_0^T u dt \tag{I.2}$$

The averaged fluctuation is zero:

$$\bar{u'} = 0 \tag{I.3}$$

I.2.2 Compressible Navier-Stokes Equations

The Navier–Stokes equations are presumed in below; where we include the turbulence in the flow. These equations are non-linear for turbulent flows and leads to interactions between fluctuations of all system parameters in all directions. The Navier–Stokes equations are given in the following [18, 19, 20]:

The Mass Conservation Equation:

$$\frac{\partial \rho}{\partial t} + \frac{\partial (\rho u_\alpha)}{\partial x_\alpha} = 0 \tag{I.4}$$

Where;

α=1,2,3

Momentum Equations:

$$\frac{\partial (\rho u_\beta)}{\partial t} + \frac{\partial (\rho u_\alpha u_\beta)}{\partial x_\alpha} = -\nabla p + \nabla \tau + \rho \sum_i y_i f_i \tag{I.5}$$

Where;

$$\alpha = 1,2,3 \; and \; \beta = 1,2,3$$

Energy Conservation Equation

$$\frac{\partial (\rho e)}{\partial t} + \frac{\partial (\rho u_\alpha e)}{\partial x_\alpha} = -\nabla (pu) + \nabla (\tau . u) + \sum_i \rho V_i y_i h_i - k \nabla T + q_R \tag{I.6}$$

q_R: Radiative heat flux vector.

The aerothermal flow equations, in cartesian coordinates, can be presented in matrix as the following [21, 22]:

$$\frac{\partial Q}{\partial t} + \frac{\partial F_1}{\partial x_1} + \frac{\partial F_2}{\partial x_2} + \frac{\partial F_3}{\partial x_3} = s \tag{I.7}$$

with:

S : Source term.

Q : Conserved variables.

F : Field describes the rate of the conserved variables.

Where:

$$Q = \begin{pmatrix} \rho \\ \rho u_1 \\ \rho u_2 \\ \rho u_3 \\ \rho e \end{pmatrix} \tag{I.8}$$

The total energy defined here for the ideal gas:

$$\rho e = \rho C_v T + \frac{1}{2}\rho(u_1^2 + u_2^2 + u_3^2) \tag{I.9}$$

If we neglect the effect of gravity, the flow F_i is written $\forall i \in \{1,2,3\}$:

$$F_i = \begin{pmatrix} \rho u_i \\ \rho u_i u_1 - \sigma_{i1} \\ \rho u_i u_2 - \sigma_{i2} \\ \rho u_i u_3 - \sigma_{i3} \\ \rho e u_i - u_j \sigma_{i1} - \lambda \dfrac{\partial T}{\partial x_i} \end{pmatrix} \tag{I.10}$$

$\lambda = \rho C_p k$: Thermal conductivity.

κ : Thermal diffusivity.

Component σ_{i1} the stress tensor presented can be written for a Newtonian fluid as [21, 23]:

$$\sigma_{i1} = -p\delta_{ij} + 2\mu A_{ij} \tag{I.11}$$

And:

$$A_{ij} = \frac{1}{2}\left[\frac{\partial u_j}{\partial x_i} + \frac{\partial u_i}{\partial x_j} - \frac{2}{3}(\nabla u)\delta_{ij}\right] \tag{I.12}$$

A_{ij}: Deformation tensor.

The substitute of the means of deformation tensor of Eq (I.10):

$$F_i = \begin{pmatrix} \rho u_i \\ \rho u_i u_1 + \rho\delta_{i1} - 2\mu A_{i1} \\ \rho u_i u_2 + \rho\delta_{i2} - 2\mu A_{i2} \\ \rho u_i u_3 + \rho\delta_{i3} - 2\mu A_{i3} \\ (\rho e + p)u_i - 2\mu u_j A_{ij} - \lambda \dfrac{\partial T}{\partial x_i} \end{pmatrix} \tag{I.13}$$

To start using the empirical relationship of Sutherland to present the viscosity:

$$\mu = \mu(273{,}15)\left(\frac{T}{273{,}15}\right)\frac{1 + T_0/273{,}15}{1 + T_0/T} \tag{I.14}$$

With:

$$\mu(273{,}15) = 1{,}711.10^{-5} Pl$$

$$T_0 = 110{,}4K$$

In the case *T<120K* using an extension of the previous law:

$$\mu\,(T) = \mu(120)\left(\frac{T}{120}\right) \tag{I.15}$$

Viscosity and thermal conductivity are connected by the Prandtl number which characterizes the thermal properties of the fluids:

$$Pr = \frac{v}{k} = \frac{C_p \mu(T)}{\lambda} \tag{I.16}$$

The thermodynamic state equation is given by:

$$P = \rho RT \tag{I.17}$$

It recalled that $R = C_p - C_v = 287{,}06 J.kg^{-1}K^{-1}$ in air at room temperature, and $\gamma = C_p / C_v$

I.2.3 The Kolmogorov Theory

The Kolmogorov theory(1942) [16] consist to use the statistical method in turbulent flows. The content of this theory is based on the Richardson's energy cascade process. Whereof, the large Reynolds numbers generate the nonlinear term, how they are dominating the viscosity according to the dimensional analysis. But this theory is valid only for the large-scale structures. The small scales are characterized by the uniqueness of the length scale (RANS). In the cascade energy, the inertial term is responsible for the transfer of energy to smaller and smaller scales. The small scales, hence, are reached for which viscosity become important [24, 25, 26].

According to this theory the vortexes in the flow have a size between the two important length scales [19]:

- Length scales ℓ: When the Reynolds number is large enough, all of the small-scale statistical properties are uniquely and universally determined by the length scale ℓ, the mean dissipation rate (per unit mass) ε and the viscosity ν.
- Length scales η: "When the Reynolds number is infinitely large, all small-scale statistical properties are uniquely and universally is independent of ν and solely determined by the length scale ℓ and the mean dissipation rate ε".

The ratio between ℓ and η is as following [27]:

$$\ell/\eta = Re^{3/4} \tag{I.18}$$

Re: is the Reynolds number.

Where;

$$E(k) = Re^{-5/3} \tag{I.19}$$

Between the short eddy scale (η) and large scale (ℓ), the idea of LES model is based on the filter equations in the space application. Structures that are larger than the cutoff frequency of the filter are explicitly represented by equations; while smaller structures are modeled (figure I.3).

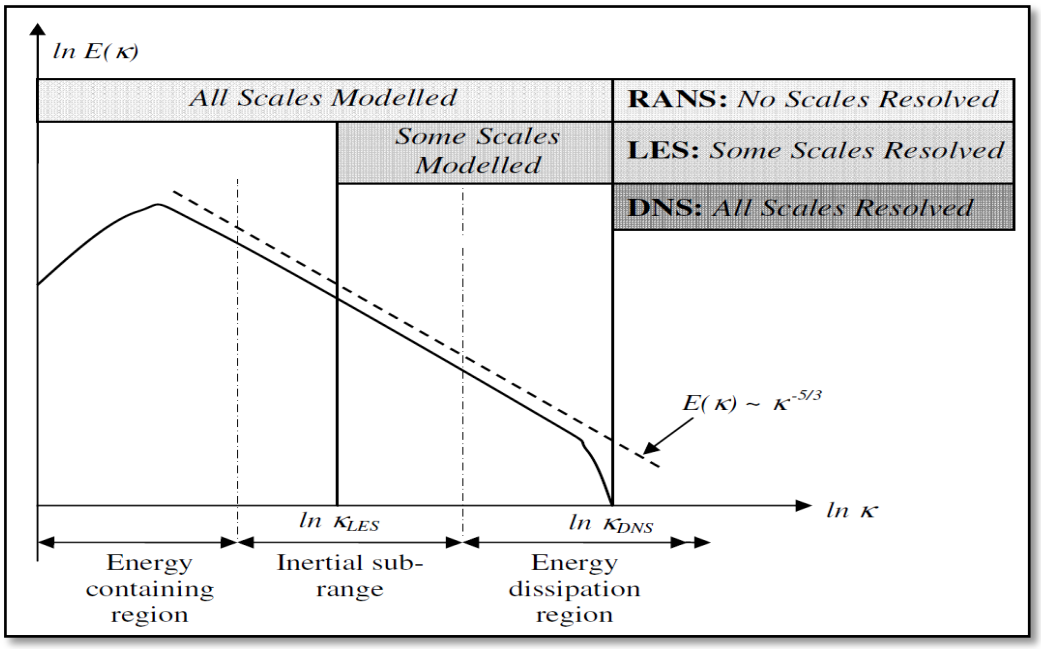

Figure I.3 Representation of DNS, LES and RANS with Kolmogorov energy spectrum, Energy E(k) related to a wave-number k [28].

I.3 Turbulent Dynamics Model

I.3.1 Large Eddy Simulation

The use of multi-scales in the turbulent flows simulation needs to precede the Large Eddy Simulation (LES) model. The fundamental idea of LES model is appeared in 1926 [29], when it is applied to many turbulent combustion systems: improve the reactive system, pollutants predictions, combustion instabilities...

LES is a computational model, where the large eddies are computed directly, while small scale vortexes are modeled. Another important concept of the LES model leads to filter the flow velocity in the turbulent case. The turbulent variables are separated to resolve and to model the fluctuations for sub-grid fluctuations [16].

We consider a variable *f* and $\overline{f}$ is there filtering used in LES. In the case of a turbulent flow quantities per unit mass are best described by a Favre, defined by [30,31]:

$$\tilde{f} = \frac{\overline{\rho f}}{\bar{\rho}} \tag{I.20}$$

The system of equations defined above (Eq I.4 & Eq I.17) becomes:

$$\frac{\partial \bar{Q}}{\partial t} + \nabla \bar{F} = \bar{s} \tag{I.21}$$

$$\bar{Q} = (\bar{\rho}, \bar{\rho}\tilde{u}_1, \bar{\rho}\tilde{u}_2, \bar{\rho}\tilde{u}_3, \bar{\rho}\tilde{e})^T \tag{I.22}$$

The total energy filtered can be written as:

$$\overline{\rho e} = \bar{\rho}\tilde{e} = \bar{\rho} C_v \tilde{T} + \frac{1}{2}\overline{\rho(u_1^2 + u_2^2 + u_3^2)} \tag{I.23}$$

The filtered flow $\overline{F}_i$ therefore:

$$\bar{F}_i = \begin{pmatrix} \bar{\rho}\tilde{u}_\iota \\ \overline{\rho u_\mathrm{i} u_1} + \bar{\rho}\delta_{i1} - 2\overline{\mu A_{\mathrm{i}1}} \\ \overline{\rho u_\mathrm{i} u_2} + \bar{\rho}\delta_{i2} - 2\overline{\mu A_{\mathrm{i}2}} \\ \overline{\rho u_\mathrm{i} u_3} + \bar{\rho}\delta_{i3} - 2\overline{\mu A_{\mathrm{i}3}} \\ \overline{(\rho e + p)u_\mathrm{i}} - 2\overline{\mu u_\mathrm{j} A_{\mathrm{ij}}} - \lambda\overline{\frac{\partial \mathrm{T}}{\partial \mathrm{x_i}}} \end{pmatrix} \tag{I.24}$$

i=1,2,3 and j=1,2,3.

I.3.2 The Governing Equations of LES

After the filtration, The equation are written as [32,33]:

Continuity:

$$\frac{\partial \bar{\rho}}{\partial t} + \frac{\partial (\bar{\rho}\tilde{u}_i)}{\partial x_i} = 0 \tag{I.25}$$

Momentum:

$$\frac{\partial (\bar{\rho}\tilde{u}_i)}{\partial t} + \frac{\partial \left(\bar{\rho}\tilde{u}_i\tilde{u}_j\right)}{\partial x_i} = -\frac{\partial}{\partial \mathrm{x_i}}\left[\bar{\rho}(\overline{u_\mathrm{i}u_\mathrm{j}} - \tilde{u}_i\tilde{u}_j)\right] - \frac{\partial \bar{\mathrm{p}}}{\partial \mathrm{x_j}} + \frac{\partial \overline{\tau_{\mathrm{ij}}}}{\partial \mathrm{x_i}} \tag{I.26}$$

Energy:

$$\frac{\partial (\bar{\rho}\tilde{h})}{\partial t} + \frac{\partial \left(\bar{\rho}\tilde{u}_i\tilde{h}\right)}{\partial x_i} = -\frac{\partial}{\partial \mathrm{x}_i}\left[\bar{\rho}(\overline{u_\mathrm{i}h} - \tilde{u}_i\tilde{h})\right] + \frac{\partial \bar{\mathrm{p}}}{\partial \mathrm{t}} + \frac{\partial \overline{u_j\tau_{\mathrm{ij}}}}{\partial \mathrm{x}_i} \tag{I.27}$$

Thermodynamic state:

$$\bar{P} = \bar{\rho}R\tilde{T} \tag{I.28}$$

$\overline{u_\mathrm{i}u_\mathrm{j}} - \tilde{u}_i\tilde{u}_j$: Reynolds tensions of sub-grid.

$\bar{\rho}(\overline{u_\mathrm{i}h} - \tilde{u}_i\tilde{h})$: Heat flow sub-grid.

- The filtered viscous stress tensor is defined by [34, 35, 36]:

$$\bar{\tau}_{\mathrm{ij}} = 2\bar{\rho}v(\tilde{S}_{ij} - \frac{1}{3}\delta_{ij}\tilde{S}_{ll}) \tag{I.29}$$

$$i = 1,2,3 \; and \; j = 1,2,3$$

Where: $\tilde{S}_{ll}$ is the sub-grid kinetic energy.

- Also, the filtering is applied on the tensor velocity of deformation as follows:

$$\tilde{S}_{\mathrm{ij}} = \frac{1}{2}\left(\frac{\partial \tilde{\mathrm{u}}_j}{\mathrm{dx}_i} + \frac{\partial \tilde{\mathrm{u}}_i}{\mathrm{dx}_j}\right) \tag{I.30}$$

I.3.3 Sub-grid Scale Models for LES

Sub-grid scale (SGS) models are used in LES to account for the unresolved part of the solution. The Smagorinsky model (1963) [37] is certainly the simplest and most commonly used eddy viscosity model of LES & SGS models. Effective viscosity is designed based on the calculation of eddy viscosity [19].

The Smagorinsky model is based on the Boussinesq hypothesis, according to which small scales of motion have shorter time scales than the large energy carrying eddies. The Boussinesq hypothesis linking the unresolved stress tensor τ_{ij} (Eq I.29) to the tensor velocity deformation $\tilde{S}_{ij}$ (Eq I.30) through a turbulent viscosity μ_T [23, 28, 38, 39, 40].

$\bar{\tau}_{ij}$ is modeled as:

$$\bar{\tau}_{ij} = 2\mu_T(\tilde{S}_{ij} - \frac{1}{3}\delta_{ij}\tilde{S}_{ll}) \quad \text{(I.31)}$$

The choice of model explain the turbulent viscosity $\mu_T = \bar{\rho}\nu_T$.

I.3.4 WALE Model

The last considered SGS closure is the Wall Adapting Local Eddy Viscosity (WALE) SGS model proposed by Nicoud and Ducros [40]. The WALE model is the most capable of representing the mean secondary flow statistics. The Smagorinsky model by construction gives a non zero value for μ_T as soon as there is a velocity gradient. Near the wall however the turbulent fluctuations are damped so that $\mu_T \rightarrow 0$. This model is used to correct a defect in the Smagorinsky model which over-estimates the turbulent viscosity in the near wall and this because the gradients due to the boundary layer [39, 41, 42].

This method takes into account the energy of the flow structures small to large transfer. But it requires the use of limiters to limit values. In addition, this model is more complex to implement than those presented here, especially on unstructured meshes. The WALE model has been developed to improve [23, 39, 43].

- The decrease of the wall.

- The transition to turbulence.

A better way to build a better operator is to consider the traceless symmetric part of the square of the velocity gradient tensor [41]:

$$\tilde{S}_{ij}^{d} = \frac{1}{2}\left(\tilde{g}_{ij}^{2} + \tilde{g}_{ji}^{2}\right) - \frac{1}{3}\tilde{g}_{kk}^{2}\delta_{ij} \tag{I.32}$$

Where the velocity gradient tensor $\tilde{g}_{ij}^{2}$ is:

$$\tilde{g}_{kk}^{2} = \frac{\partial u_i}{\partial x_i} \tag{I.33}$$

so the expression for Eddy viscosity is:

$$v_T = (C_w\Delta)^2 \frac{\left(S_{ij}^{d}S_{ij}^{d}\right)^{3/2}}{\left(\tilde{S}_{ij}^{d}\tilde{S}_{ij}^{d}\right)^{5/2} + \left(S_{ij}^{d}S_{ij}^{d}\right)^{5/4}} \tag{I.34}$$

where C_w is a WALE constant model. A simple way to determine this constant is to assume that the new model gives the same ensemble-average Sub-grid kinetic energy dissipation as the classical Smagorinsky model. Thus one obtains [41]:

$$C_w^2 = C_s^2 \frac{\langle\sqrt{2}(\bar{S}_{ij}\bar{S}_{ij})^{3/2}\rangle}{\langle\bar{S}_{ij}\bar{S}_{ij}\overline{OP}_1/\overline{OP}_2\rangle} \tag{I.35}$$

C_s: Smagorinsky constant.

Cw can be assessed numerically using several fields of homogeneous isotropic turbulence. According Nicoud and Ducros, constant *Cw* varies little according to the configuration (unlike *Cs* in the Smagorinsky model). The value of *Cw* = 0.49. $\nu_T = 0$ if the flow is two-dimensional. Moreover, a strongly related to the spatial operator used in the Smagorinsky model [23,39,44]:

$$\overline{\mathrm{OP}}_1 = (\mathrm{S_{ij}^{d}S_{ij}^{d}})^{3/5} \tag{I.36}$$

$$\overline{\mathrm{OP}}_2 = (\bar{\mathrm{S}}_{\mathrm{ij}}\bar{\mathrm{S}}_{\mathrm{ij}})^{5/2} + (\mathrm{S_{ij}^{d}S_{ij}^{d}})^{5/4} \tag{I.37}$$

The Eddy viscosity is defined as [41]:

$$v_T = (\mathrm{C_w}\Delta)^2 \frac{\overline{\mathrm{OP}_1}}{\overline{\mathrm{OP}_2}} \tag{I.38}$$

I.4 Probability Density Function Model for Combustion

Probability density Function (PDF) method is used in turbulent combustion for the first time by Cook and Riley in 1994 [45]. PDF plays an important role to surmount the closure in the scalars variables in the governing equations of the reactive system. The fundamental idea of the PDF method is based on describing the statistical property of thermo-chemical variables, where the average value of a thermo-chemical scalar variable is obtained by weighting the instantaneous value with a PDF for the mixture fraction [28, 46].

I.4.1 Properties of PDF

The PDF can be defined as the derivative of the cumulative distribution function, i.e. [47]:

$$P(y) = \lim_{\Delta y \to 0} F(y)/\Delta y \tag{I.39}$$

Where:

F(y): is the probability function.

In turbulence reactive flow contain N chemical species, we need to consider a set of N composition variables $y \equiv \{y_1, y_2, ...y_N\}$. PDF has the following properties [14]:

Property 1:

$$P(y) \geq 0 \tag{I.40}$$

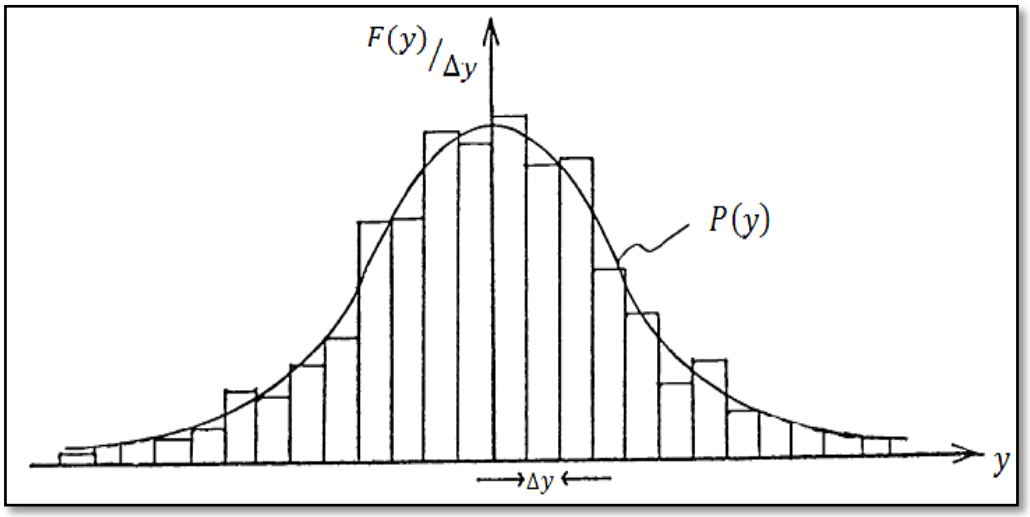

Figure I.4 Histogram together with it' s limiting PDF [14].

Property 2:

Since $\lim_{y\to-\infty} F(y)=0,$ and $\lim_{y\to+\infty} F(y)=1,$ then

$$\int_{-\infty}^{+\infty} P(y)dy = 1 \tag{I.41}$$

Where, the integration $dy = dy_1 dy_2 \ldots\ldots dy_N$ is over the whole of composition space [48].

If $1 \geq y \geq 0$ then [44, 49]:

$$\int_{0}^{1} P(y)dy = 1 \tag{I.42}$$

Property 3:

The PDF has to be non-negative with a compact support and the integral of it has to equal 1. The expectation Q(y) is defined as [47]:

$$\bar{Q} = \langle Q \rangle = \int_{-\infty}^{+\infty} P(y)Q(y)dy \tag{I.43}$$

If the PDF is known, the mathematical expectation and the math central of any function of the random variable can be calculated. In particular the mean $\bar{y}$ and the math central $\overline{y''^2}$ can be determined.

The density is given by the function $\rho(y)$ which can be written by (Eq I.43) is [43, 50]:

$$\bar{\rho} = \langle \rho(x,t) \rangle = \int P(y;x,t)\, \rho(y)dy \tag{I.44}$$

Where the integration occurs on all values of the set y. $P(y;x,t)$ is the possibility to obtain the values included between y and $y+dy$ in point x and moment t [51].

For variable density flows Favre averages are usually preferred:

$$\tilde{Q} = \frac{\overline{\rho Q}}{\bar{\rho}} = \int_{-\infty}^{+\infty} Q(y)\bar{P}(y)dy \tag{I.45}$$

And Favre-decomposition into mean and fluctuation is defined as [52]:

$$Q = \tilde{Q} + Q'' \tag{I.46}$$

Q" : the Favre-fluctuation.

It is also useful to define the Favre-PDF by:

$$\tilde{P}(y) = \frac{\overline{\rho(y)P(y)}}{\bar{\rho}} \tag{I.47}$$

The aim of models of turbulent combustion is to determine the average rate of the chemical reaction. The appreciation of the average rate of chemical production is not direct and must be based on a phenomenological approach. We will use a progress variable of reaction c defined such that [44, 49, 53]:

- c = 0 in the unburned reactants
- c = 1 in the products

And the fraction of mixture Z introduced here is

- Z=0 in oxidant pure
- Z=1 in pure fuel

Statistical properties of f intermediate states of the scalar fields in turbulence can be deduced from the PDF [22, 54]:

$$\bar{y} = \int_0^1 yP(y;x,t)dy \text{ and } \overline{y''^2} = \int_0^1 (y-\bar{y})^2 P(y;x,t)dy \tag{I.48}$$

With reference to simplifying assumptions outlined by Klimenko (1990) and Bilger (1993) [29], they proposed the use closings for these averages, this seems step suitable for the non-premixed flames at stoichiometric conditions optimize [51, 54].

I.4.2 The Beta-PDF Approach

In this work we use the Beta PDF(Cook and Riley 1994) [55]. It has been evaluated as a model for sub-grid mixture fraction fluctuations in LES. Where the probability function is written as:

$$P(x;a,b) = x^{a-1}(1-x)^{b-1}\frac{\Gamma(\mathrm{a}+\mathrm{b})}{\Gamma(\mathrm{a})\Gamma(\mathrm{b})} \tag{I.49}$$

Where the parameters a and b are related to the distribution mean and variance (μ ,σ^2) by:

$$a = \frac{\mu(\mu - \mu^2 - \sigma^2)}{\sigma^2} \qquad (I.50)$$

$$b = \frac{(1-\mu)(\mu - \mu^2 - \sigma^2)}{\sigma^2}$$

When applied to mixture fraction, x⟶Z, μ ⟶ $\tilde{Z}$ and σ^2⟶$\widetilde{Z''^2}$

I.4.3 Non-Premixed Combustion Modeling

Non-premixed combustion is one of the combustion types, which is fuel and oxidizer in the reaction zone. In this mode individual species transport equations are not solved. Rather than that, transport equations for one or two conserved scalars (the mixture fractions) are solved and individual component concentrations are derived from the predicted mixture fraction distribution. This approach has been specifically developed for the simulation of turbulent diffusion flames. In the Non-Premixed Combustion Model, turbulence effects are accounted for with the help of an assumed shape PDF [56].

I.4.4 Progress Variable

The progress variable is a combination of an intermediate and a product species. The progress variable is better interpreted as a step function that separates unburnt mixture and burnt gas in a given flow field (figure I.5). It is therefore related to the spatial structure of the flame front and its statistics rather than to a reacting scalar such as the temperature or the reactants and products. Turbulent closure of the source term of the progress variable is based on a model for the turbulent flame rate. This property of c becomes more evident when the PDF of *c* at a given location x is considered. It is introduced as [43, 44, 57, 58]:

$$c = \frac{T - T_0}{T_{eq} - T_0} \qquad (I.51)$$

The progress variable *c* is defined as a normalized product mass fraction [44]:

$$c = \frac{Y_p}{Y_p^{eq}} \qquad (I.52)$$

It is possible to make combinations between the chemical species:

$$c = \frac{Y_{p1} + Y_{p2}}{Y_{p1}^{eq} + Y_{p2}^{eq}} \tag{I.53}$$

Where Y_P is the mass fraction of productions.

The transport equation gives the progress variable *c* may be in the form [54, 59]:

$$\frac{\partial(\bar{\rho}\tilde{c})}{\mathrm{dt}} + \frac{\partial(\bar{\rho}\tilde{u}_i\tilde{c})}{\mathrm{dx_i}} = \frac{\partial}{\mathrm{dx_i}}(\bar{\rho}a_c\frac{\partial}{\mathrm{dx_i}}\tilde{c}) + \overline{\rho\,\omega_c} \tag{I.54}$$

Where:

i=1, 2, 3

a_c is the diffusion coefficient.

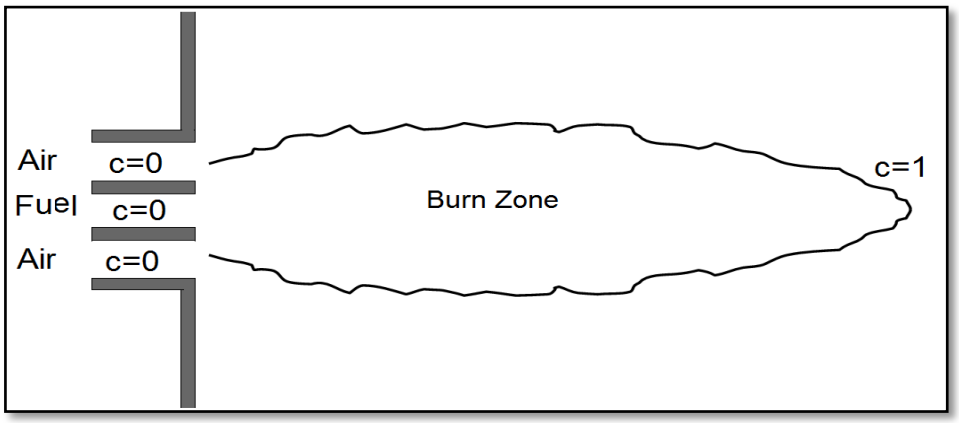

Figure I.5 Schematics of the progress variable distribution in the combustion.

I.4.5 Mixture Fraction Equation

The role of mixture fraction in non-premixed combustion is the description of the transport of conserved scalars parameters based on the inflow mixing streams The mixture fraction is a conserved scalar variable, which means that a conservation equation for the mixture fraction will have no source term. The basis of the non-premixed modeling approach is that under a certain set of simplifying assumptions, the instantaneous thermo-chemical state of the fluid is related to a conserved scalar quantity known as the mixture fraction(Z) [47, 55, 60].

Conservation equations can be reduced to the solution of a single transport equation for the mixture fraction. All the species mass fractions and temperature can then be calculated from mixture fraction concentrations using functional relationships. This forms the basis of the conserved scalar approach [28,44, 48, 49].

$$\frac{\partial(\bar{\rho}\tilde{Z})}{\partial t}+\frac{\partial(\bar{\rho}\tilde{u}_i\tilde{Z})}{\partial x_i}=\frac{\partial}{\partial x_i}(\bar{\rho}a_c\frac{\partial\tilde{Z}}{\partial x_i}) \quad \text{(I.55)}$$

With:

$$i=1,2,3$$

This scalar is passive, there are no source terms of chemical reaction, the first term of left border of equation is unsteady and the second is the convection. The right border represented the molecular diffusion [44, 49, 53].

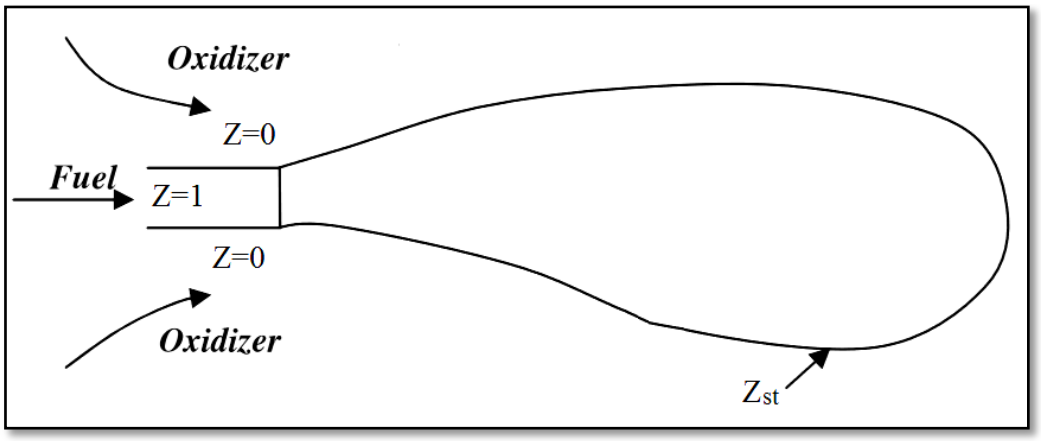

Figure I.6 Surface of stoichiometric mixture (Z_{st}) for a turbulent jet diffusion flame [28].

Conclusion

In this chapter, we dealt with the idea for turbulent non-premixed combustion modeling. Where, the turbulence is a complicate status of flows that needs to precede a new methods and models to resolve the problem in this flow status. The considering of the combustion complicates more system. For this reason, we use LES to describe the turbulence by statistical methods in the Navier-Stokes equations to describe correctly the structure of turbulent flows. In LES, the effects of the small turbulent motions are modeled, and the larger ones are computed. The PDF methods are used to resolve the closure problem in the thermo-chemical terms in the governing equations of turbulent combustion.

CHAPTER II

Numerical Study of Combustion by CFD

CHAPTER II Numerical Study of Combustion by CFD

Computational Fluid Dynamics codes play an important role in the design and the optimization of the flows processes. CFDs are created by the numerical methods for the solutions of the set of governing equations describing the system. Also, they are given as tools to present the details that the experimental can't give. The combustion process is described by the set equations that govern the transport equations for the fluid dynamics, the heat transfer and the chemical reactions. Moreover, the details of the flow are added in the CFD considering the combustion case with chemical multispecies and with multi-scales of flow.

The aim of this chapter is to give the main steps of the simulation and the modeling of the combustion of the two types of the flues (Methane and Bio fuel): configuration, meshes, equations ...

II.1 Computational Fluid Dynamics

A Computational Fluid Dynamics (CFD) is a tool, that we can use to study the fluid behavior accompanied with chemical reaction, heat transfer and mass transfer. The computer science progress has an impact on the CFD efficiency with the integration of the complex equations: conservation of mass, momentum, energy and chemical species [61, 62, 63, 64]:

- Meshing the geometry.
- Applying the governing equations on the cells of the computational domain.
- Using the algebraic form of equations.

The common steps in the CFD applications can be summarized in the Figure II.1.

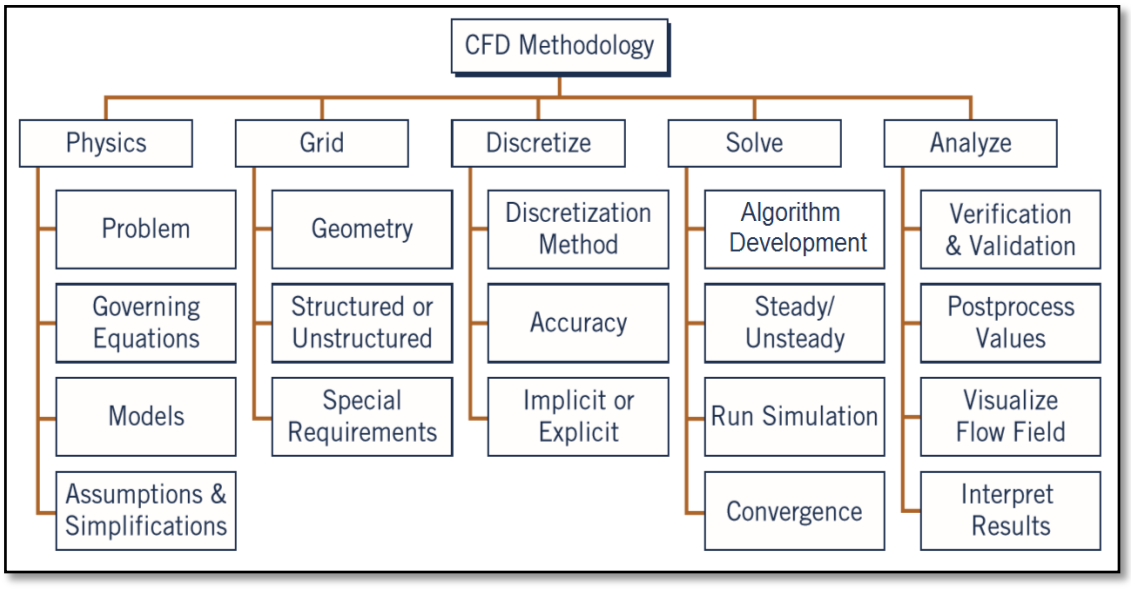

Figure II.1 Flow chart general CFD methodology[65].

II.2 Fluent CFD

To do this, we use a software package, it includes three major components:

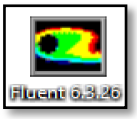

FLUENT & 

GAMBIT & 

Exeed

In this research, FLUENT 6.3.26 software is used to achieve the modeling and simulation. The pre-processor used to construct the model grid is GAMBIT 2.2.30.

II.2.1GAMBIT

GAMBIT software is used for the illustration of the configuration and establishing the pre-processing phase of modeling i.e. drawing the model (for geometry modeling and mesh generation), constructing the grid and defining the boundaries and zones. GAMBIT was designed to help in analyzing and designing of mesh building models for CFD and other scientific applications. GAMBIT receives user input primarily by means of its graphical user interface (GUI) [56, 66].

II.2.2 FLUENT

FLUENT is one of the widely used CFD software package. Which is designed for numerical simulations of various kinds of flows. Furthermore, it treats the problem and then gives the result [64].

II.2.3 EXEED

EXEED execute GAMBIT (which is designed for Linux system) in the Windows system.

II.3 Steps for CFD Analysis

II.3.1 Step 01: Creating And Meshing Basic Geometry

This step illustrates geometry creation and mesh generation for a simple geometry using GAMBIT. The most important elements of GAMBIT for drawing the combustion chamber is the row of three buttons at the top right to control the various operations (figure II.2):

(1) Geometry: Used to create various two and three-dimensional shapes for the problem.

(2) Mesh: Used to mesh the geometry into smaller areas/volumes for use in numerical solution methods.

(3) Zones: Used to define boundaries and continuum types.

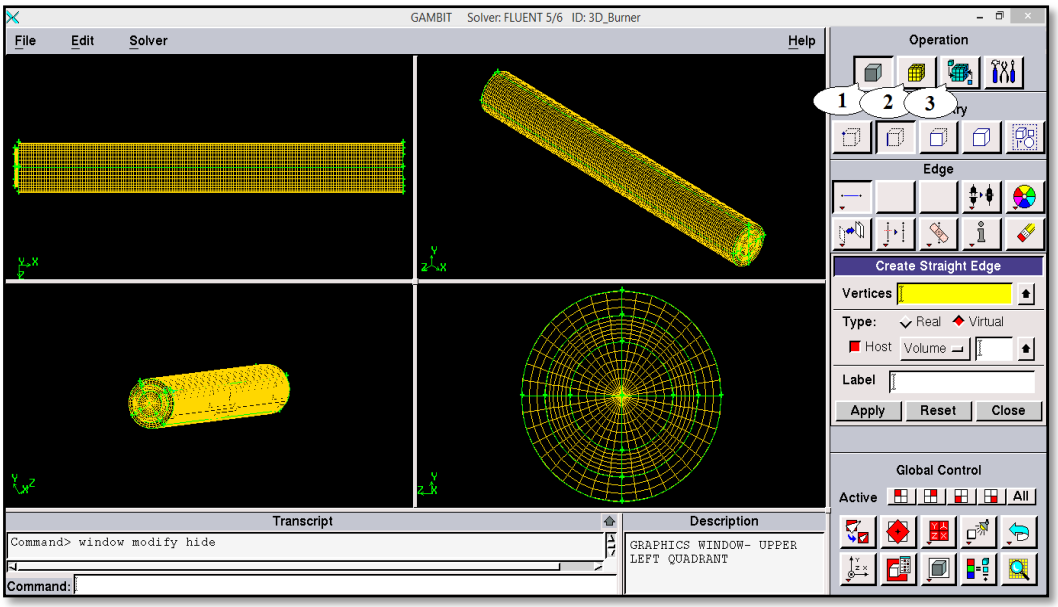

Figure II.2 Combustion chamber design by GAMBIT.

II.3.2 Step 02: Opening FLUENT

Start the 3DDP (three-dimensional double precision) version of FLUENT.

3ddp → Run

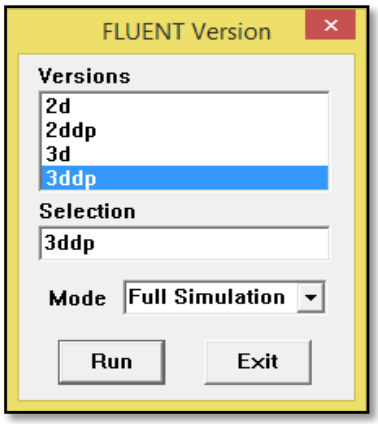

Figure II.3 Window starting FLUENT version.

II.3.3 Step 03: Grid

1. Read the Case file

File → Read → Case

Go to the directory where you saved your mesh file is saved and open the file with extension .msh.

2. Check the grid

Grid → Check

- For further confirmation, under the Display menu choose Grid. This will open the Grid Display window.
- Click on the Display icon.

3. Scale the grid

Grid → scale

- Under units conversion, select cm from the drop-down list to complete the phrase "Grid was created in cm".
- Click Scale to scale the grid. The reported values of the Domain Extents will be reported in the default SI units of meters.

4. Display of grid

Display → Grid

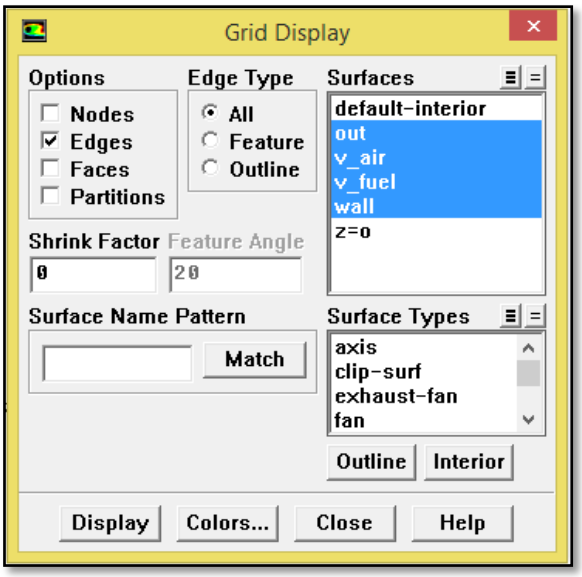

Figure II.4 Grid display.

- Retain the default settings.
- Click Display to view the grid in the graphics display window (Figure II.5).

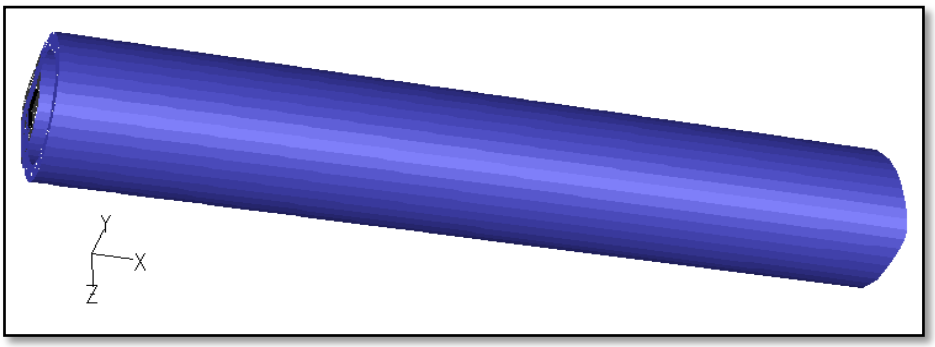

Figure II.5 Graphic Display of Grid.

II.3.4 Step 04: Define Solver Properties

1. Retain the default solver settings

Define → Models → Solver

Define the domain as axisymmetric, and keep the default (segregated) solver.

2. Enable heat transfer by activating the energy equation:

Define → Models → Energy

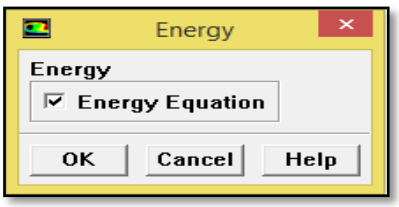

Figure II.6 Energy Equation solution.

The energy equation needs to be turned on since this is a compressible flow where the energy equation is coupled to the continuity and momentum equations.

3. Select the standard LES turbulence model:

Define → Models → Viscous

4. Select the P1 radiation model:

Define → Models → Radiation

5.Select the Non-Premixed Combustion model:

Define → Models → Species → Transport & Reaction

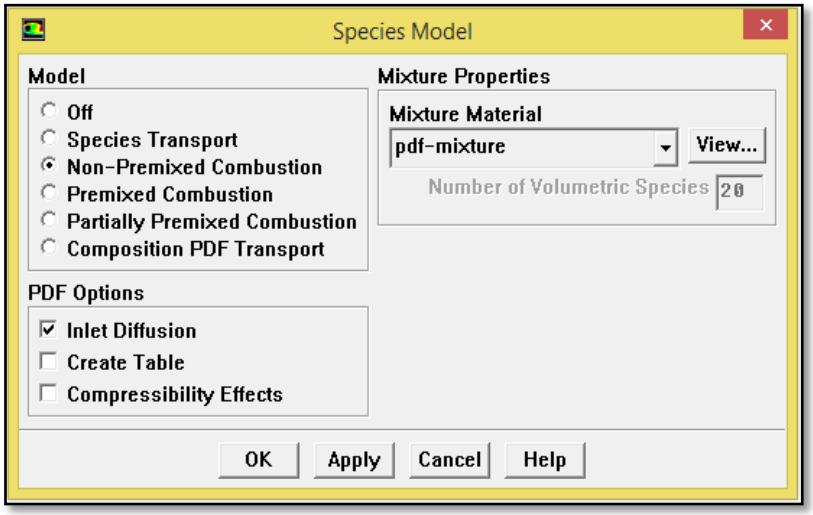

Figure II.7 Definition of Transport & Reaction model**.**

- Under Model, select Non-Premixed Combustion.
- Under PDF Options, turn on Inlet Diffusion.
- In the Mixture Material drop-down list under PDF-mixture.

II.3.5 Step 05: Define Material Properties

II.3.5.1 Mixture Materials

The concept of mixture materials has been implemented in FLUENT to facilitate the setup of species transport and reacting flow. A mixture material may be thought as a set of species and a list of rules governing their interaction. The mixture material carries with it the following information:

- A list of the constituent species, referred to as “fluid” materials
- A list of mixing laws dictating how mixture properties (density, viscosity, specific heat, etc.) are to be derived from the properties of individual species if composition dependent properties are desired
- A direct specification of mixture properties if composition-independent properties are desired
- Diffusion coefficients for individual species in the mixture
- Other material properties (absorption and scattering coefficients) that are not associated with individual species.
- A set of reactions, including a reaction type (finite-rate, eddy dissipation, etc.) and stoichiometry and rate constants [67].

Define material properties for heat transfer:

Define → Materials

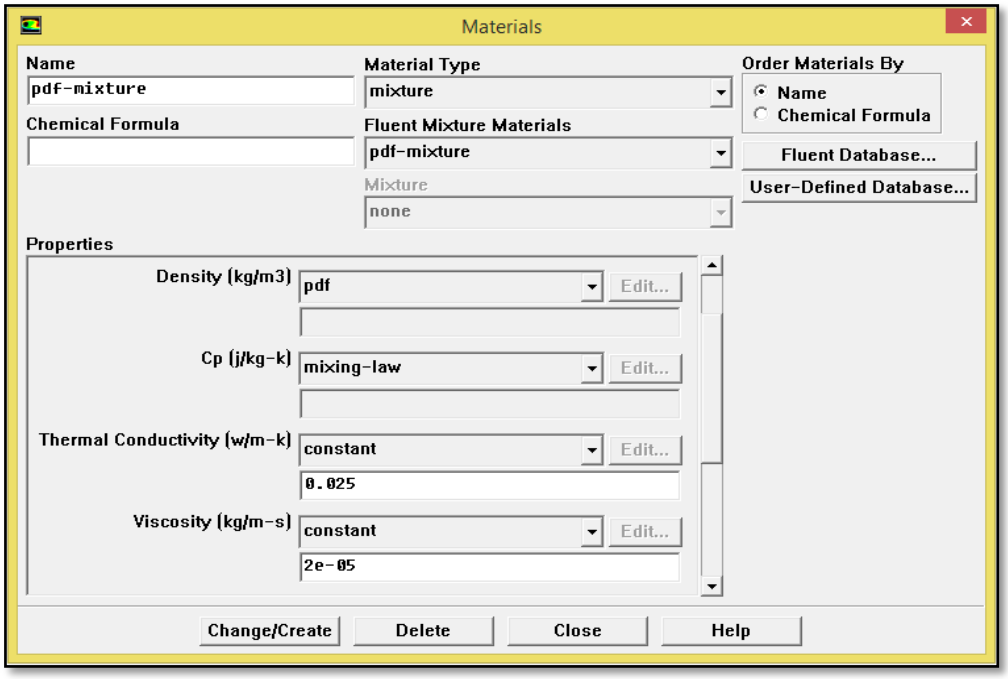

Figure II.8 Materials Window.

II.3.6 Step 06: Define Boundary Conditions

Set boundary conditions for the following surfaces: inlet, outlet, wall …

Boundary conditions must be properly specified. Either over- or under specifying boundary conditions will lead to an inaccurate solution. A proper formulation requires [68]:

- governing equations.
- boundary conditions.
- coordinate system specification.

Define the boundary conditions for the zones (Figure II.9):

Define → Boundary Conditions

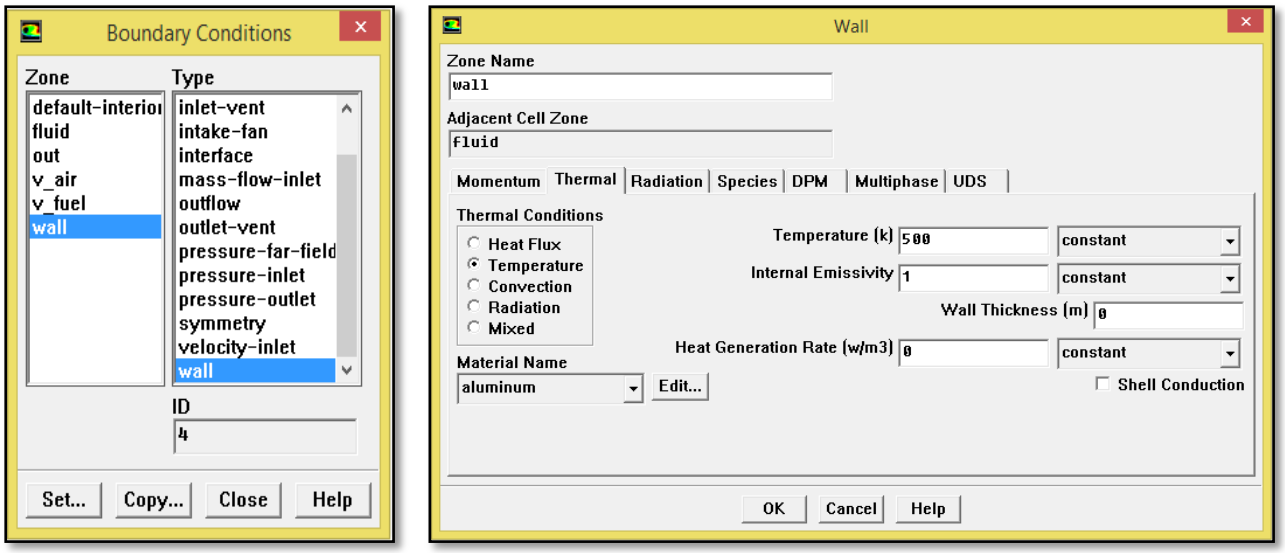

Figure II.9 Boundary conditions of wall temperature.

- Select wall from the Zone list.
- Select wall from the Type list.
- Click the Thermal tab.
- Select Temperature from the Thermal Conditions list.
- Enter 500 K for Temperature.
- Enter 1 for Internal Emissivity.
- Click OK to close the Wall panel.

II.3.7 Step 07: Non Adiabatic PDF Table

1. Select the Non-Premixed Combustion model.

Define → Models → Species

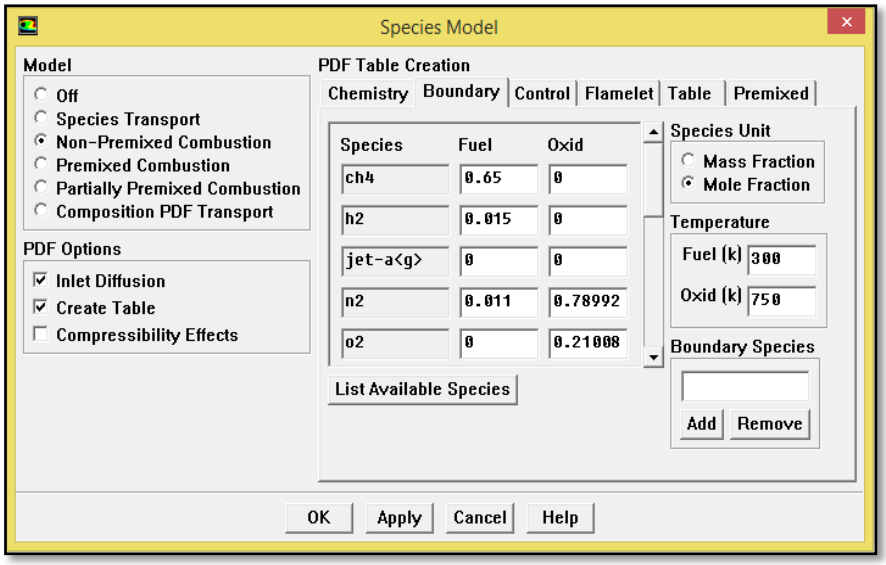

Figure II.10 The Species Panel.

- Select Create Table.
- Click the Boundary tab to add and define the boundary species (Figure II.11).

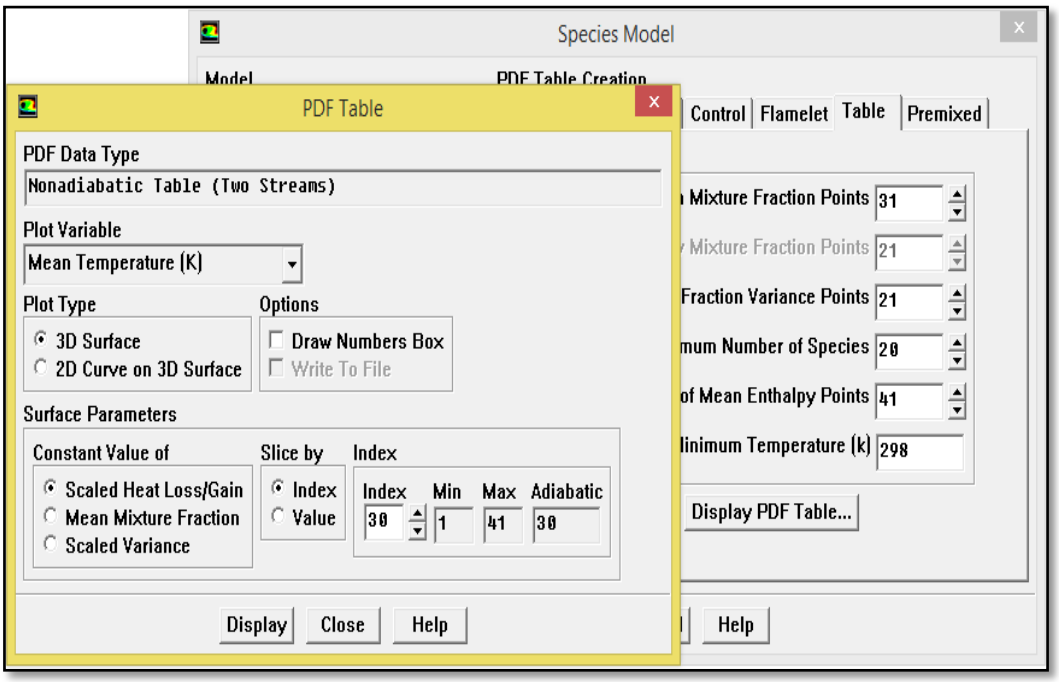

Figure II.11 Mean temperature as function for average mixture fraction.

- Click the Table tab to specify the table parameters and calculate the PDF table.
- Click the display Table… button to open the PDF Table dialog box.
- click display, we get the following (Figure II.12):

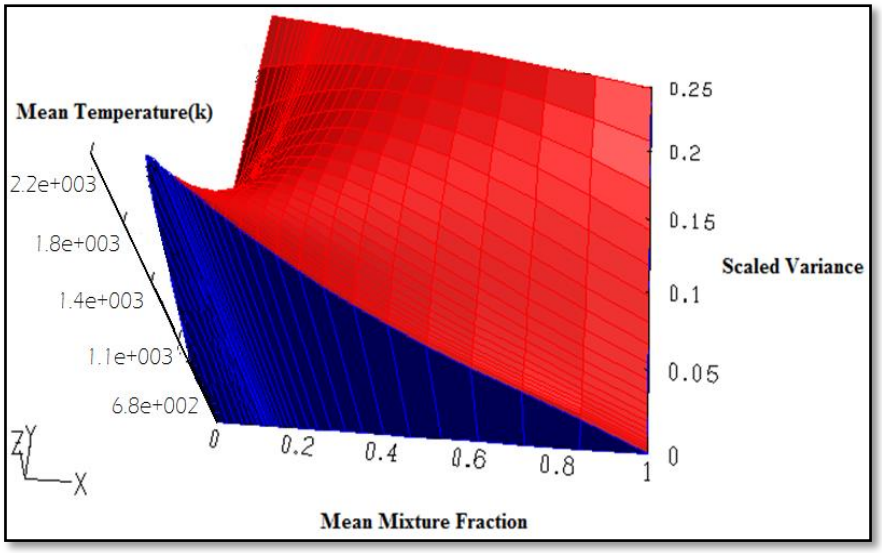

Figure II.12 Temperature solutions from the equilibrium chemistry library for the Bio fuel combustion.

II.3.8 Step 08: Solution

1. Set Solution Controls.

Solve → Controls → Solution

The default under-relaxation factors are considered to be too aggressive for reacting flow cases with high swirl velocity. For a combustion model it may be necessary to reduce the under-relaxation to stabilize the solution**.**

2. Initialize the field variables.

Solve → Initialize → Initialize

Initializing the flow using a high temperature and non-zero fuel content will allow the combustion reaction to begin. The initial condition acts as a numerical "spark" to ignite the Bio fuel air mixture.

3. Enable the display of residuals during the solution process.

Solve → Monitors → Residual

4. Write case (---.cas)

File → Write → Case

5. Iterate Until Convergence

Solve → Iterate

Enter a value of 0.0002 for the Time Step Size and enter 1000 under Number of time steps. Increase the Maximum Iterations per Time Step to 300. Click Iterate (Figure II.13).

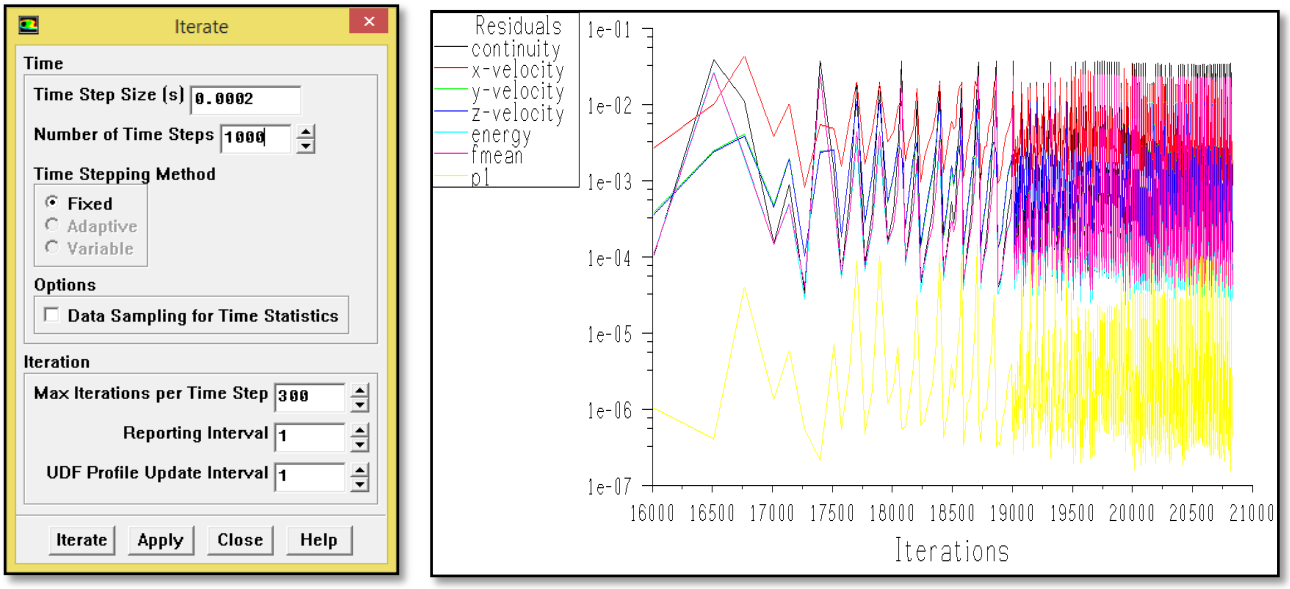

Figure II.13 Residual of the equations during the iterations.

6. Save the data file (---.dat).

File → Write → Data

II.3.9 Step 09: Analyze Results

II.3.9.1 Display Contour & Vectors

a) Temperature:

Display the predicted temperature field:

Display → contours

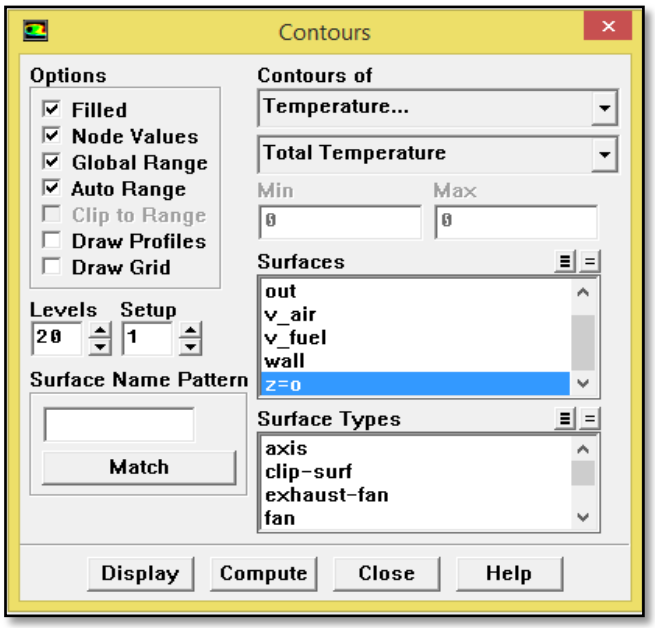

Figure II.14 Display Contour.

- Select Temperature...
- Select Total Temperature from the Contours of drop-down lists.
- Select z = 0.
- Click Display, we get the following (Figure II.15).

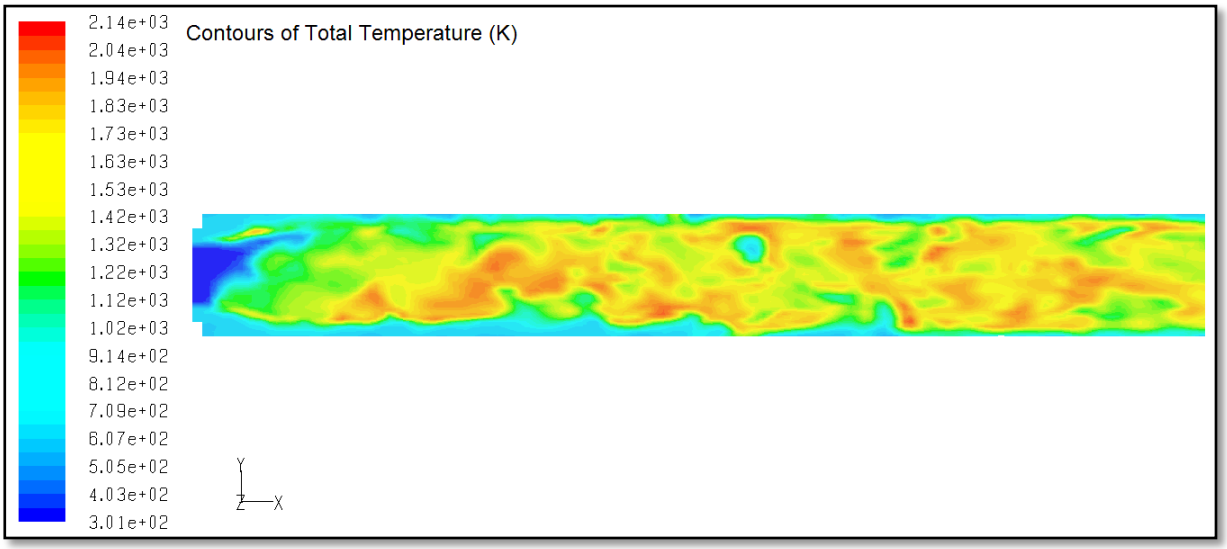

Figure II.15 Total temperature contours of Biofuel/Air.

b) CO Mass fraction:

Display the predicted CO Mass fraction

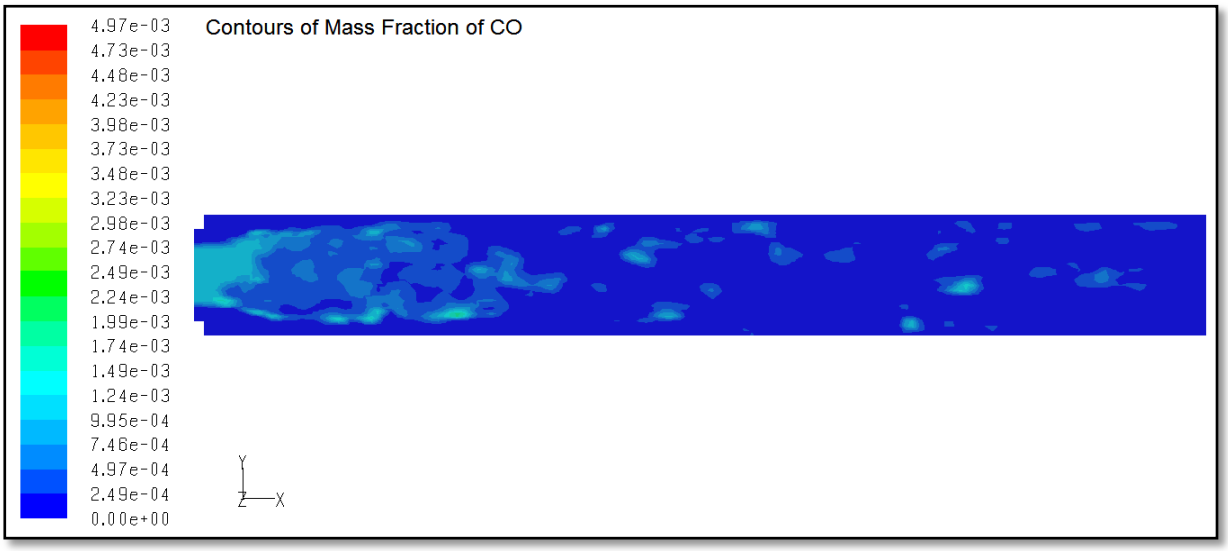

Figure II.16 CO Mass Fraction Contours of Biofuel/Air..

c) Velocity:

Display Contour of Velocity

Display → Vectors

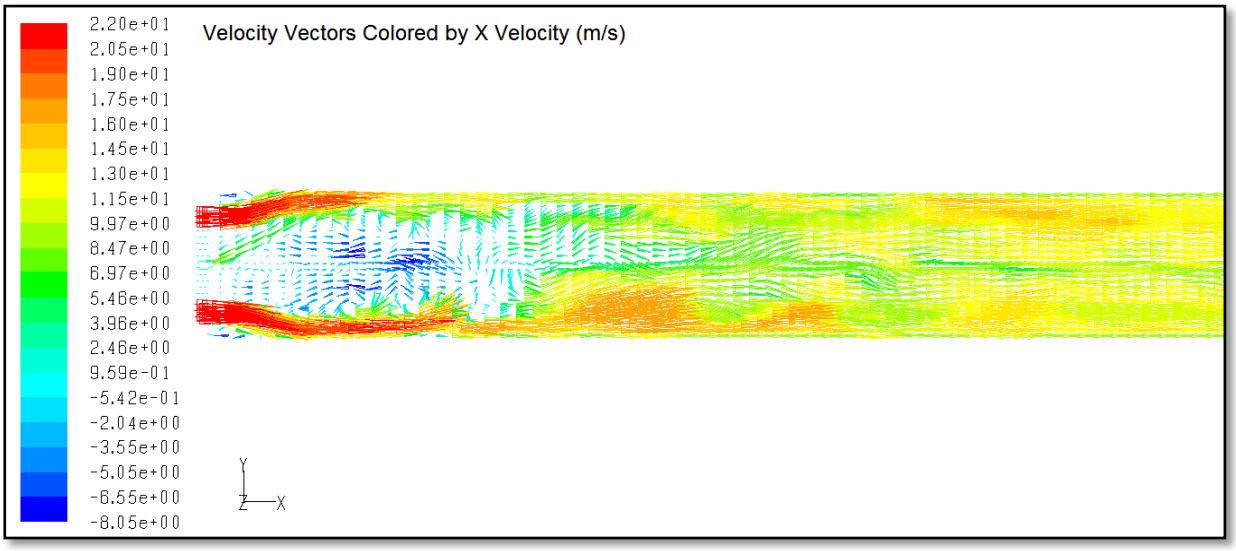

Figure II.17 X Velocity Contours of Biofuel/Air.

II.3.9.2 Drawing the graphs

Plot → XY Plot

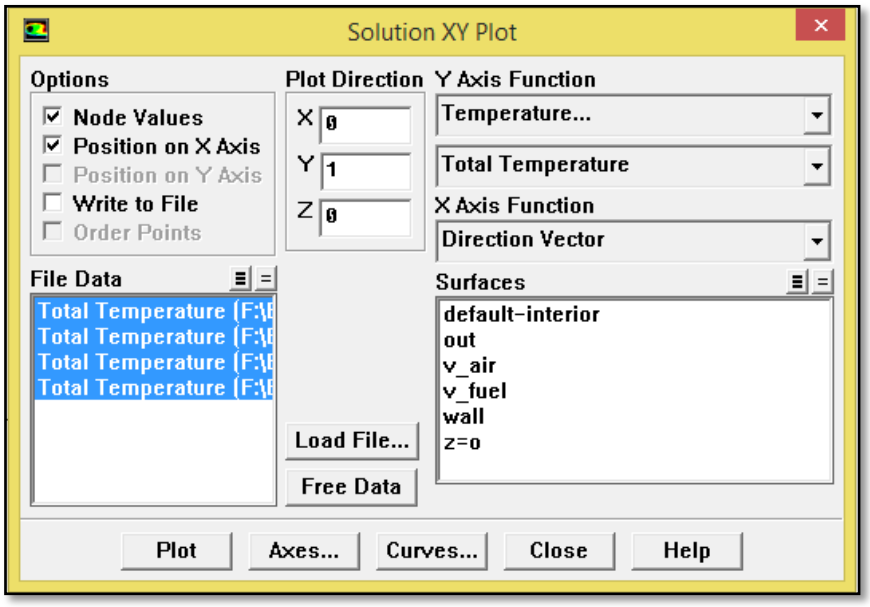

Figure II.18 Solution XY Plot panel.

- Select Temperature...
- Select Total Temperature from the Contours of drop-down lists.
- Select surfaces from the Surfaces selection list or File Data.
- Click Plot, we get the following (Figure II.19).

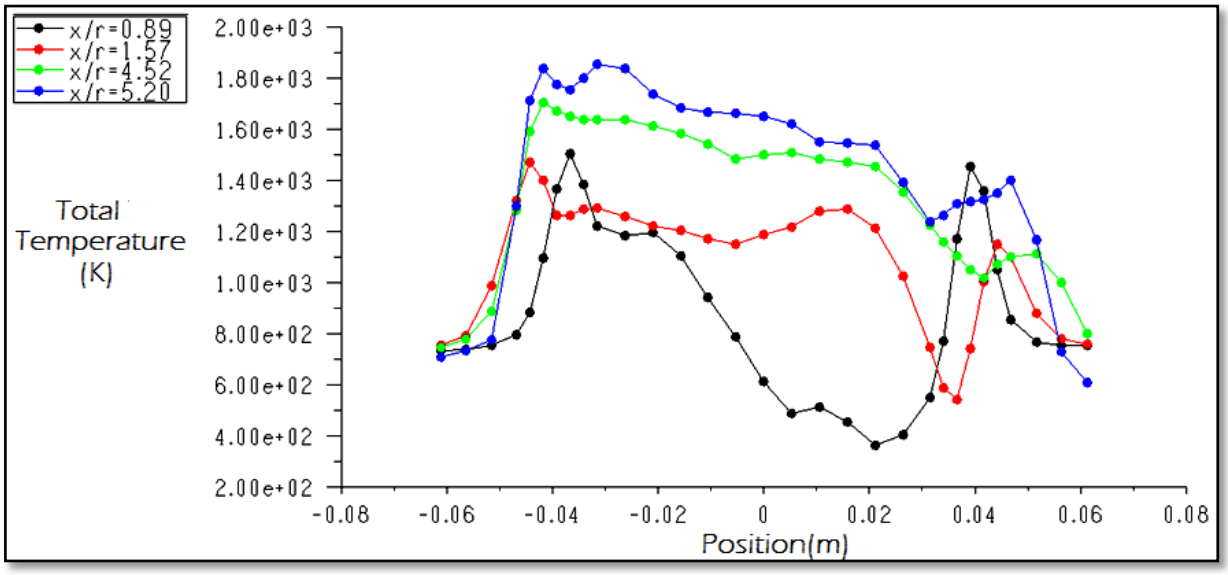

Figure II.19 Plot of Total Temperature.

Conclusion

In the present study, CFD simulation tools are shown and used to investigate and to understand the Bio fuel combustion. CFD is introduced as an important tool to study and to simulate the cylindrical combustion chamber in three-dimensional supplied by the Bio fuel. Moreover, the combustion modeling is carried out by the dynamic model of turbulence Large Eddy Simulation (LES) coupled with scalar approach β-PDF including in FLUENT. In the next chapter we will discuss the obtained results and compare them with the experience.

CHAPTER III

Results & Discussion

CHAPTER III Results & Discussion

The objective of this chapter is the computation and the interpretation of the results obtained by FLUENT-CFD code for three dimensional the non-premixed turbulent combustion in cylindrical chamber supplied by two coaxial jets (Biofue/air or Methane/air). Also, in this part we validate the performance of the LES-WALE model coupled with the Beta-PDF approach with the experimental data in the same stations and the same conditions.

III.1 Experimental Configuration and Application Domain

III.1.1 The Experimental Configuration

The configuration of the two coaxial jets that confine the combustor is given in figure III.1. Where it was the focus of numerous experimental investigations because of its relatively simple geometry and its similarity to gas turbine burner [69]. Thereby, we investigated the numerical validation of the LES/PDF coupled models with the experimental data, to study the behavior of the non-premixed combustion fueled by CH_4 and Bio fuel. Whereas, the study consists of three main parameters: mean axial velocity, mean temperature and mean mass fraction of Carbone monoxide. The cylindrical combustion chamber is of ray R_4 and L in length supplied by two coaxial jets, the central one has an internal ray R_1 and an external R_2, which injects the methane with inlet mass flow rate and temperature respectively Q_1 and T_1. The annular one has an internal ray R_3, that injects the air with an inlet mass flow rate Q_2 and preheated at a temperature T_2. The combustion chamber is pressurized to 3.8 atm and has a constant temperature wall of T_{wall} [69]. The dimensions and flow conditions specified in the experiment are summarized below:

$R_3 \equiv R$ =0.04685 m	R_1=0.03157 m	Q_1 =0.0072 kg/s	T_1 =300 K	T_{wall} =500 K
R_4=0.06115 m	R_2=0.03175 m	Q_2=0.137 kg/s	T_2 =750 K	L= 1m

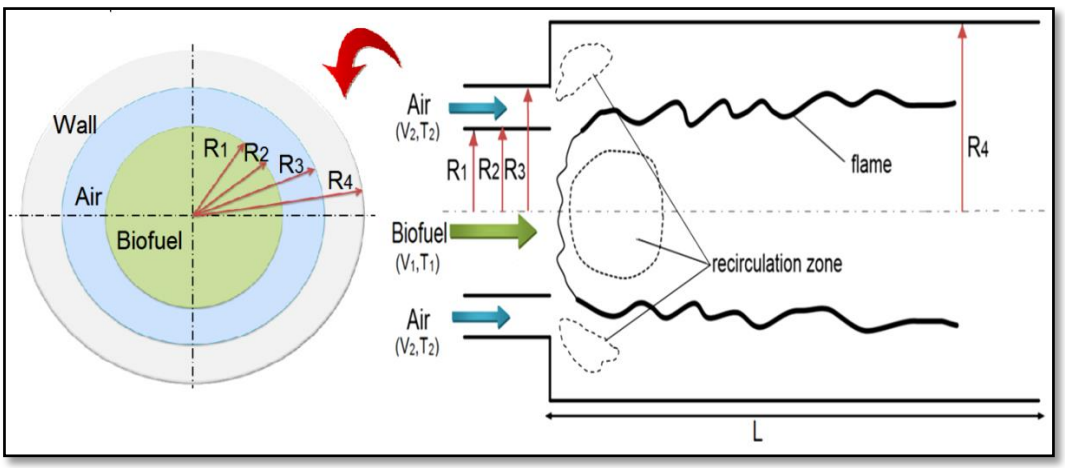

Figure III.1 Schematic of the burner [55].

The present numerical study investigates three dimension (3D) cylindrical burner. Where, the grid used for all the simulations is performed by Gambit. Therefore, the selected meshes are of parallelepipeds type; the grid is smooth and refined for both nearly solid boundaries of the burner and in the longitudinal direction in the level of interaction of air and fuel, to accommodate more information in the solid boundary and the flame zone. The volume contains approximately 2.7 million cells, the size of a cell ranges from 2.934596e-07 m^3 to 3.057304e-09 m^3.

III.1.2 Governing Equations

In this part of work, we study the behavior of a non-premixed turbulent combustion, in three dimensions using numerical simulation. We can write the governing equations for compressible flow in Cartesian coordinates as follows [33, 70]:

Continuity:

$$\frac{\partial \bar{\rho}}{\partial t} + \frac{\partial (\bar{\rho}\tilde{u}_i)}{\partial x_i} = 0 \tag{III.1}$$

Momentum:

$$\frac{\partial (\bar{\rho}\tilde{u}_i)}{\partial t} + \frac{\partial \left(\bar{\rho}\tilde{u}_i\tilde{u}_j\right)}{\partial x_i} = -\frac{\partial}{\partial \mathrm{x_i}}\left[\bar{\rho}(\overline{u_i u_j} - \tilde{u}_i\tilde{u}_j)\right] - \frac{\partial \mathrm{p}}{\partial \mathrm{x_j}} + \frac{\partial \overline{\tau_{\mathrm{ij}}}}{\partial \mathrm{x_i}} \tag{III.2}$$

Progress variable:

$$\frac{\partial (\bar{\rho}\tilde{c})}{\mathrm{dt}} + \frac{\partial (\bar{\rho}\tilde{u}_i\tilde{c})}{\mathrm{dx_i}} = -\frac{\partial \tau_c}{\partial \mathrm{x_i}} + \frac{\partial}{\mathrm{dx_i}}(\bar{\rho}a_c\frac{\partial}{\mathrm{dx_i}}\tilde{c}) + \overline{\rho\,\dot{\omega}_c} \tag{III.3}$$

Mixture fraction:

$$\frac{\partial \left(\bar{\rho}\tilde{Z}\right)}{\partial \mathrm{t}} + \frac{\partial \left(\bar{\rho}\tilde{u}_i\tilde{Z}\right)}{\partial \mathrm{x_i}} = \frac{\partial}{\partial \mathrm{x_i}}(\bar{\rho}a_c\frac{\partial \tilde{Z}}{\partial \mathrm{x_i}}) \tag{III.4}$$

Thermodynamic state:

$$\bar{P} = \bar{\rho}R\tilde{T} \tag{III.5}$$

$$i = 1,2,3 \; and \; j = 1,2,3$$

The many the sub-grid models are based on the hypothesis of Boussinesq which present the tensor of the unsolved constraints τ_{ij} to the tensor velocity of deformation $\tilde{S}_{ij}$ by the intermediary of a turbulent viscosity. The small scales influence the large scales via the SGS stress [33, 70]:

$$\bar{\tau}_{\mathrm{ij}} = 2\bar{\rho}v_T\tilde{S}_{ij} - \frac{1}{3}\bar{\rho}\tilde{K}_{ll}\delta_{ij} \tag{III.6}$$

Where k_{ll} is the subgrid kinetic energy.

The filtered strain rate tensor is defined by [33, 70]:

$$\tilde{S}_{\mathrm{ij}} = \frac{1}{2}\left(\frac{\partial \tilde{\mathrm{u}}_j}{\mathrm{dx}_i} + \frac{\partial \tilde{\mathrm{u}}_i}{\mathrm{dx}_j}\right) - \frac{1}{3}\tilde{\mathrm{u}}_{ll}\delta_{ij} \tag{III.7}$$

We selected the WALE eddy viscosity model to represent the eddy viscosity term in Eq(III.8). The main idea of this model is to recover the proper behavior of the eddy viscosity near the wall in case of wall-bounded flows, while preserving interesting properties such as the capacity to provide no eddy-viscosity in case of vanishing turbulence [71].

The major interest of this model first relies on the fact that it needs no information about the direction and distance from the wall thus being really suitable for unstructured grids, where evaluating a distance to the wall is precarious. The residual stress tensor of the WALE eddy viscosity model can be found as [72]:

$$v_t = (C_w\Delta)^2 \frac{\left(S_{ij}^d S_{ij}^d\right)^{3/2}}{\left(\tilde{S}_{ij}^d \tilde{S}_{ij}^d\right)^{5/2} + \left(S_{ij}^d S_{ij}^d\right)^{5/4}} \tag{III.8}$$

$$S_{ij}^d = \frac{1}{2}\left(\tilde{g}_{ij}^2 + \tilde{g}_{ji}^2\right) - \frac{1}{3}\tilde{g}_{kk}^2\delta_{ij} \tag{III.9}$$

$$\widetilde{g_{ij}} = \frac{\partial \tilde{\mathrm{u}}_i}{\mathrm{dx}_j} \tag{III.10}$$

Cw: WALE model constant (*Cw* =0.49). The Δ is the spatial filter width, which is generally related to the grid size of the resolved field.

We use in this work PDF approach as a SGS closure in LES of turbulent non-premixed methane and Bio fuel /air flames. The joint PDF of the SGS is determined by the solution of its modeled transport equation [33, 70, 72].

III.2 Results and Discussion

In this section, we begin with the validation of the coupled models described previously with the experimental data. Whereof, the results are validated in the same stations and that defined in the experience [55]. After that, we introduce the effect of the hydrogen fuel injection with the methane. In addition, the same parameters used for the validation are used also to control the flame behavior supplied by the CH4/H2 mixture. Moreover, the presentation and comparison of results are based on normalizing length and velocity by using, respectively, the injector radius (R≡R3) and the inlet bulk velocity of the air (U≡V2).

III.2.1 Validation of Numerical Models

III.2.1.1 Axial Velocity of CH4/Air Combustion

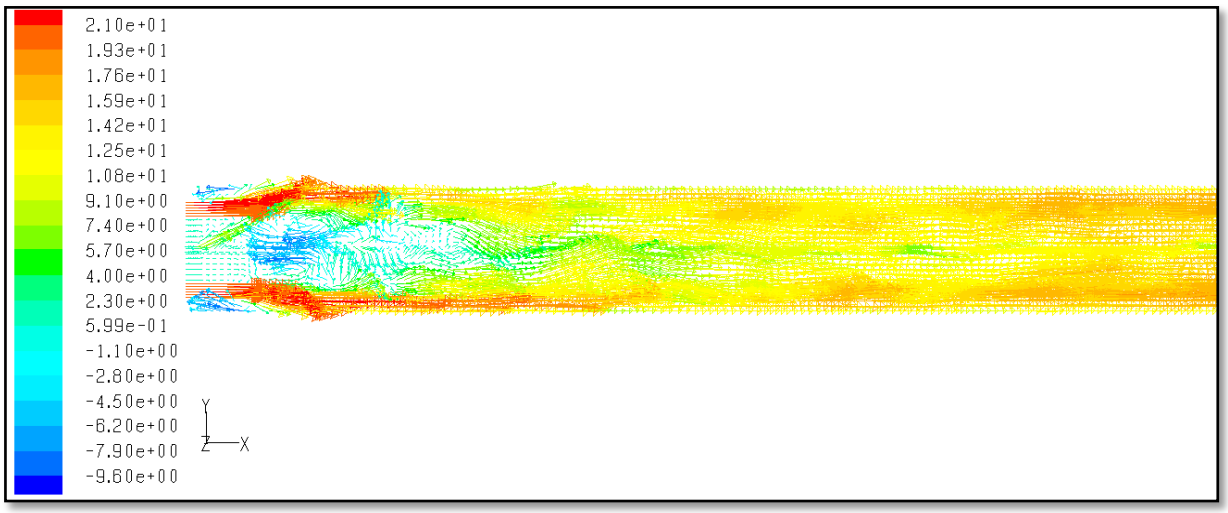

Figure III.2 Velocity (m/s) distribution in the burner of CH_4/Air combustion.

Figures III.3 illustrate the comparison of the radial profiles of the average axial velocity obtained by the computational of coupled LES_WALE/PDF models and the experimental data [55]. In fact, the numerical results achieve acceptable agreement with the experimental data. The results obtained in this study are better than previous results. Thereby, the negative values of axial velocity in the x/R=0.14, 0.38 and 1.27 present the recirculating regions. Where, we observe the formation of two recirculating zones. The first one located in the center of the burner in the fuel jet level, generated by the delayed flow of the methane. And the second one caused by the brutal change in the burner section comparatively to the coaxial jets. However, the high values of velocity are located in the flame zone that is presented by the beak (x/R=0.14, 0.38 and 1.27); where it disappeared in the last station (x/R=4.67). The divergence may be due to the fact that the fully developed fuel and air inflow conditions were assumed in the simulations. But, in the experiment the inlet flows devices were located only on short distance upstream of the burner. So, the mean relative incertitude between the computational and the experiment is given by 7 %.

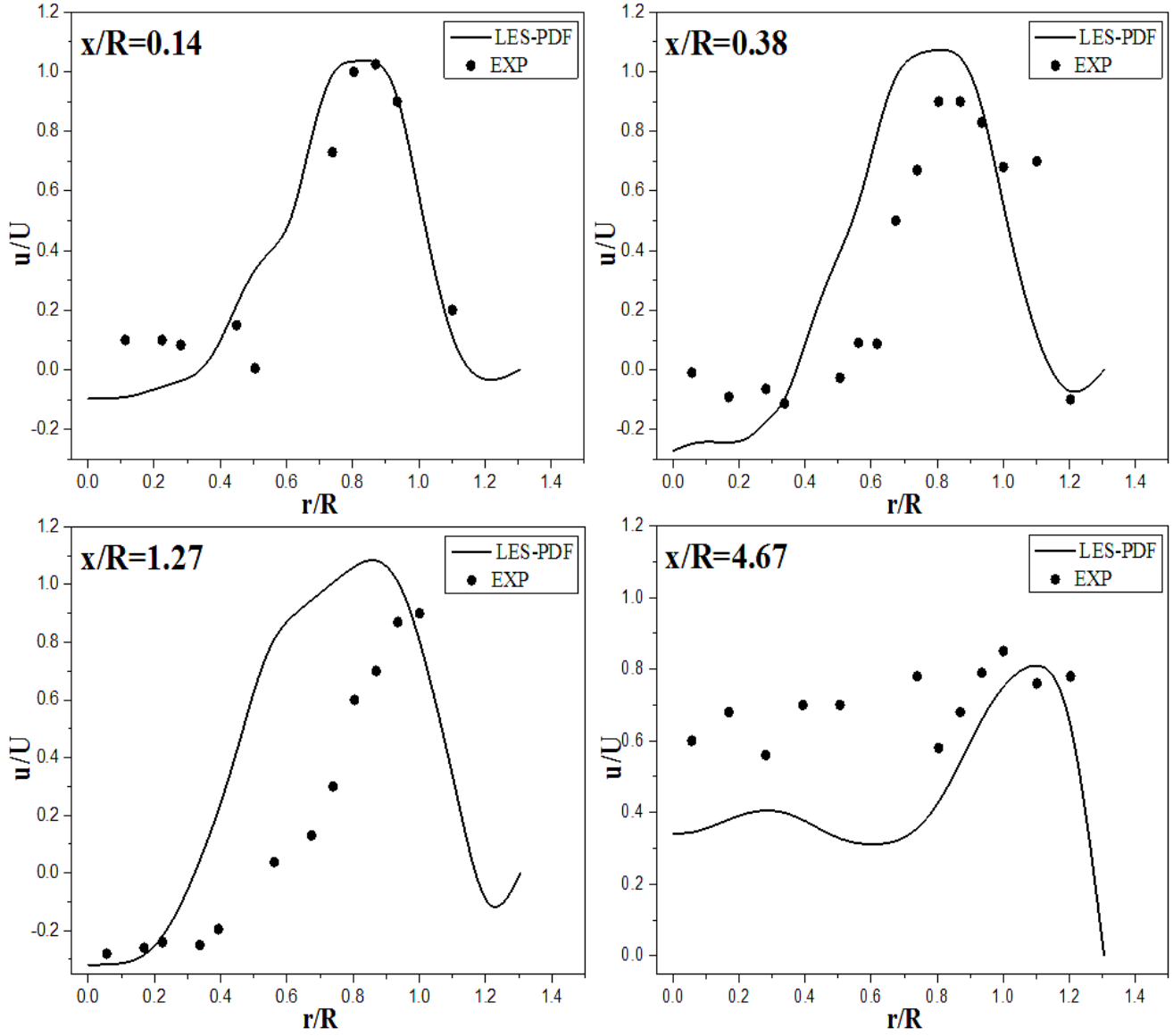

Figures III.3 Radial profiles of average axial velocity.____ Simulation (LES/PDF), •Experiment [55].

III.2.1.2 Temperature of CH_4/Air

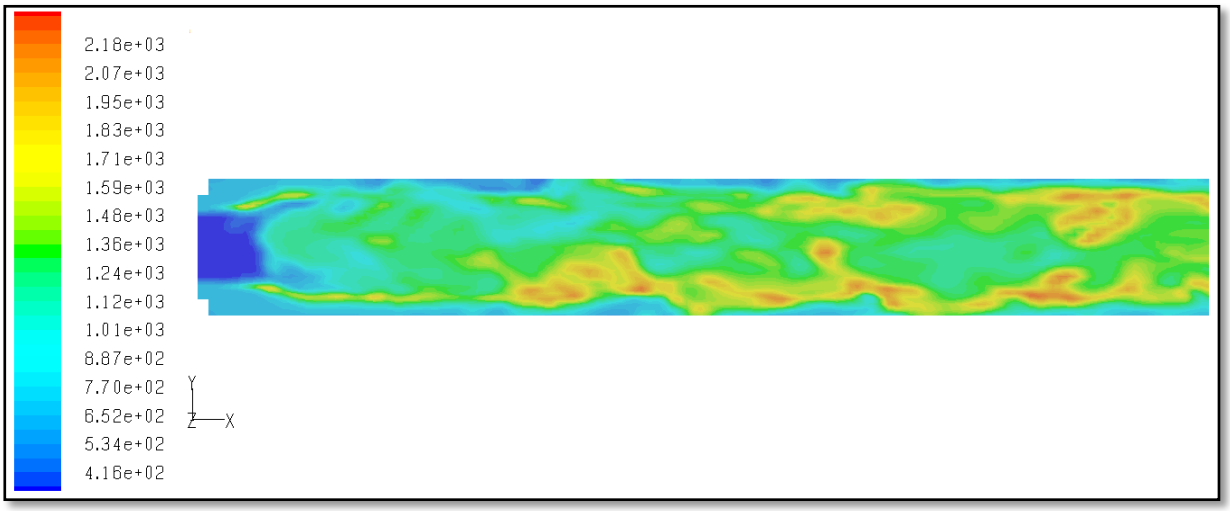

Figure III.4 Temperature (K) distribution in the burner of CH_4/Air combustion.

The comparisons of the predicted radial profiles of the average temperature with the experiments in different stations (x/R=0.89, 1.57, 4.52 and 5.20) in the burner is presented in figures III.5; both numerical and experimental profiles have almost the same tendency. Whereas, the profiles characterized by the peak that presented the flame zone, where it seated on the shear layers that is the same zone where the fuel and the air are meeting. The shearing zone is created to improve the mixture of both coaxial jets flows to supply the combustion chamber by rich mixture. Whereas, the high temperature values are located around the flame region and the temperature begins decrease with the radial distance to achieve the wall temperature. Moreover, the peak founded in the temperature profiles comes to attenuate in the downstream of the burner. The general level of agreement between simulation and experiment is satisfactory. Hereby, the comparison shows an overestimation, especially in the last station x/R=5.20. Thereby, this disagreement is due to the regions with large temperature fluctuations and difficulty to ensure perfectly the experiment condition of isothermal walls cooling with at 500K [13]. The mean of relative incertitude between the simulation and the experiment is given by 10%.

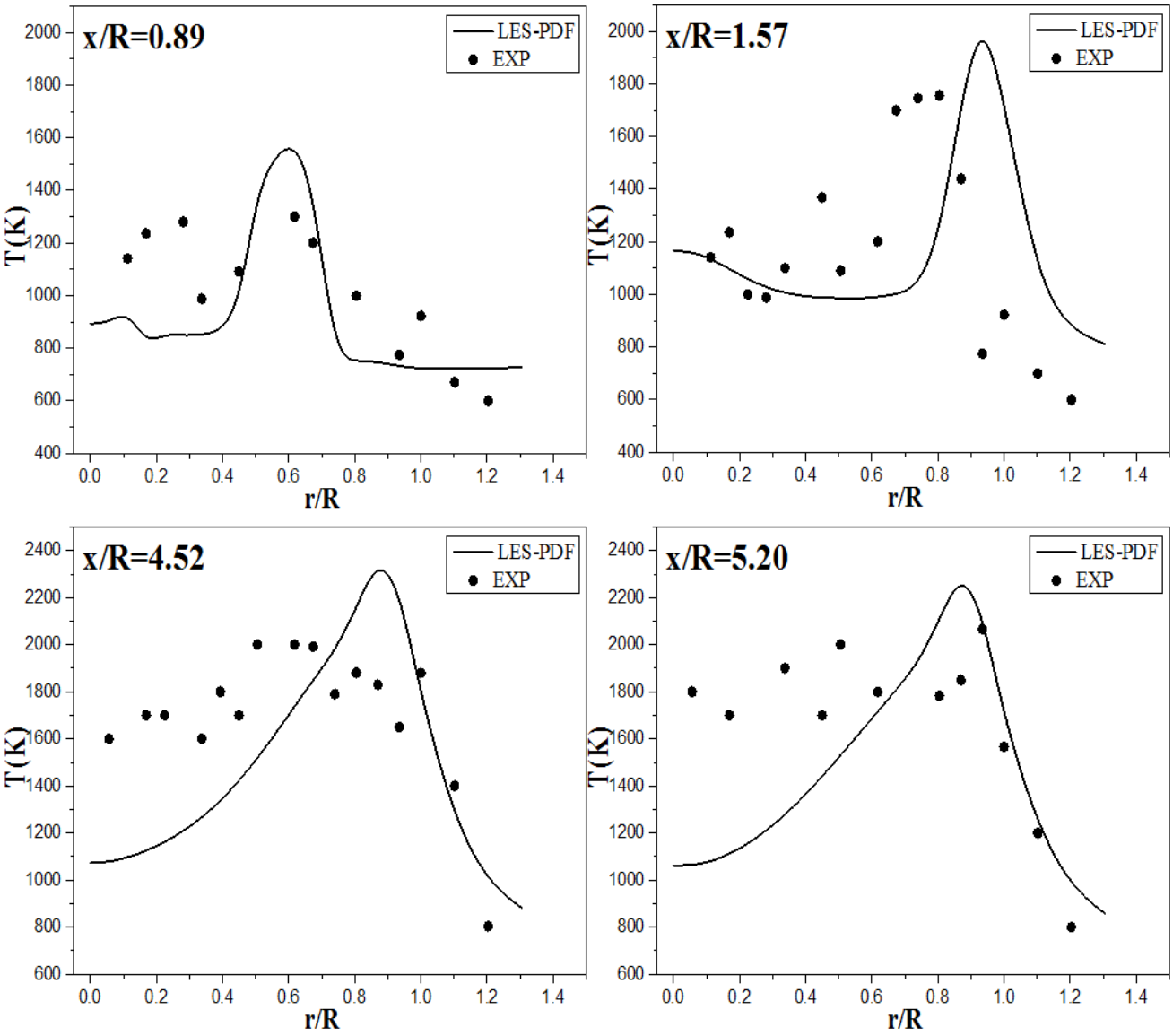

Figures III.5 Radial profiles of average temperature.____ Simulation (LES/PDF), • Experiment [55].

III.2.1.3 Carbon Monoxide Mass Fraction of CH_4

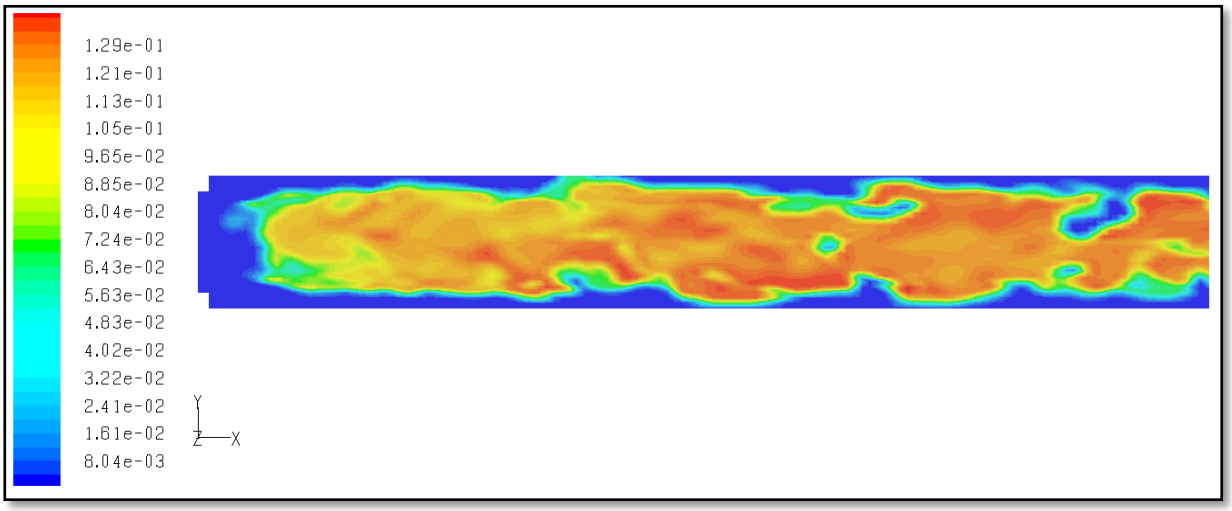

Figure III.6 CO distribution in the burner of CH_4/Air combustion.

Figures III.7 illustrate the comparison of predicted and experimental radial distribution of the carbon monoxide mass fraction for different stations in the burner. The computation predicted as well as the values of CO mass fraction comparatively to experimental data. Indeed, the height values of mass fraction of CO located in the center of the combustion chamber, which decrease when going away from the center of the burner. The profiles of CO mass fraction have the same tendency with temperature profiles which explain the high values of CO around the flame zone, the zone of reaction and production of CO. In first station, x/R=0.21, the values of CO are low relatively to the other three stations. However, in the rest stations (x/R= 3.16, 3.84 and 7.41) the mixture of methane and air is caused by the turbulence effect, that allows their mixture and burning in order to produce CO with high values. The disagreement between the numerical and the experiment is given by 5 %.

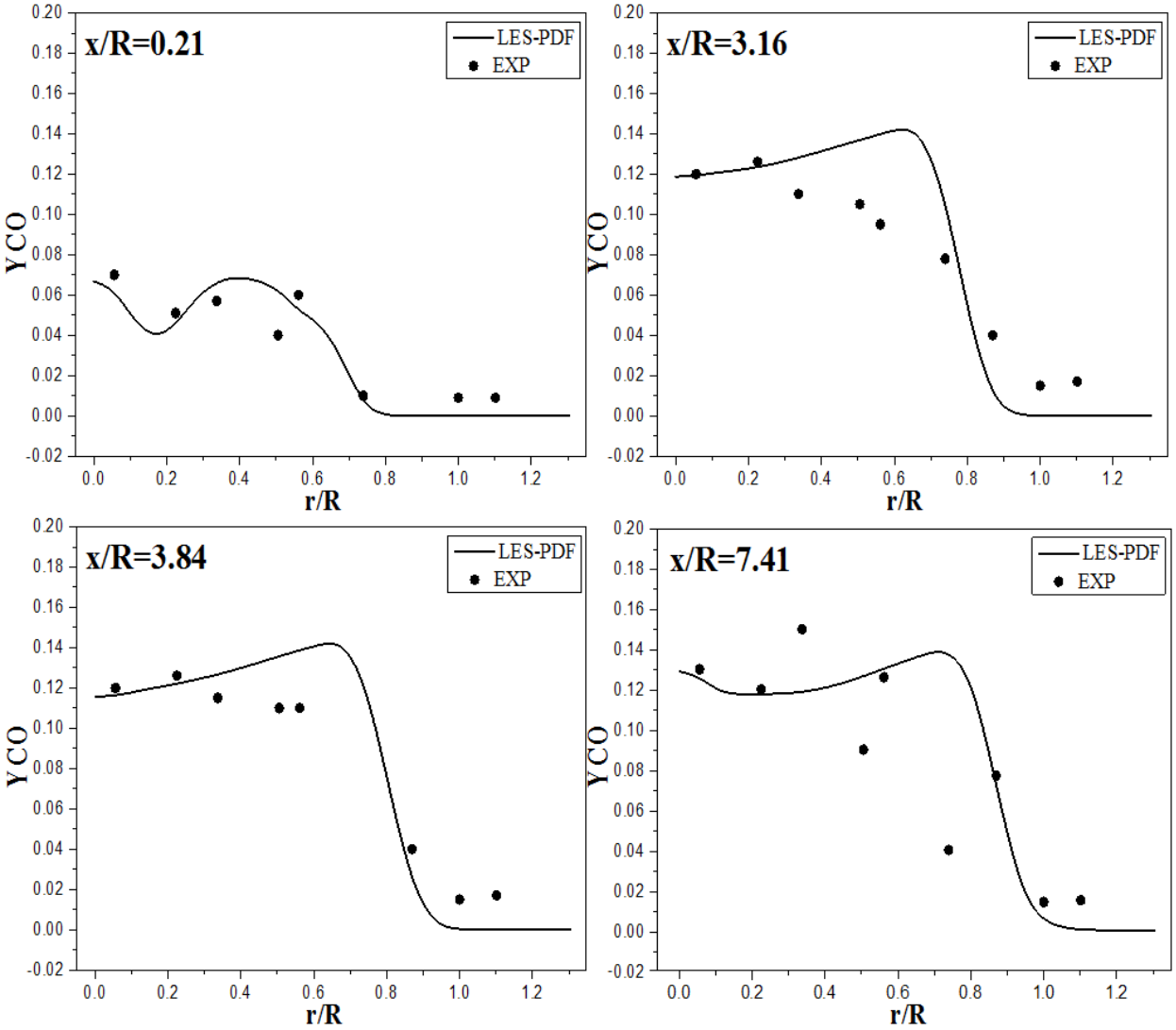

Figures III.7 Radial profiles of average Carbon monoxide. ____Simulation (LES/PDF), •Experiment[55].

III.2.2 Comparison of Bio Fuel & CH_4

III.2.2.1 Carbon Monoxide Mass Fraction

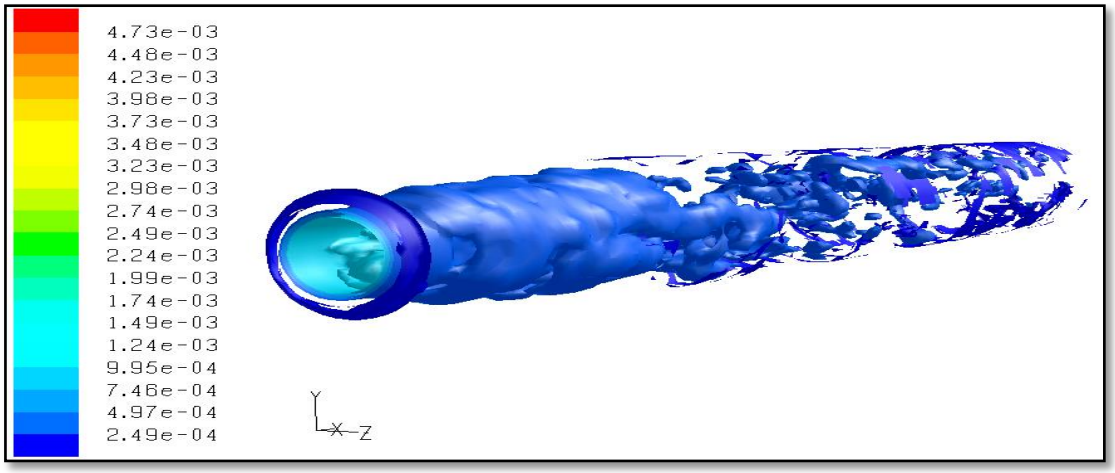

Figure III.8 CO distribution in the burner of Biofuel/Air combustion(3D).

The figures III.9 show a comparison between mass fraction of CO resulting from the combustion of CH_4 and Bio fuel. The results illustrate clearly that CO value of Bio fuel is much lower amount than fuel of methane; where the difference between the two graphs is approximately 92%. At the inlet of the combustion chamber, the value of CO is considerable especially in the first station. For the second station, x/R=3.16, the graph is characterized by the y_{co}=0.12 for CH_4, but $y_{co}\approx 0$ for the Bio fuel. In the x/R=3.84 and x/R=7.41, the CO mass fraction have same tendency with the preview station. In the outlet of the burner, the values of the CO produced by the CH_4 present the reduction of approximately of 10% relatively to the inlet stations. However, the CO produced by the combustion of Bio fuel equal to 0 in all stations of the combustion chamber.

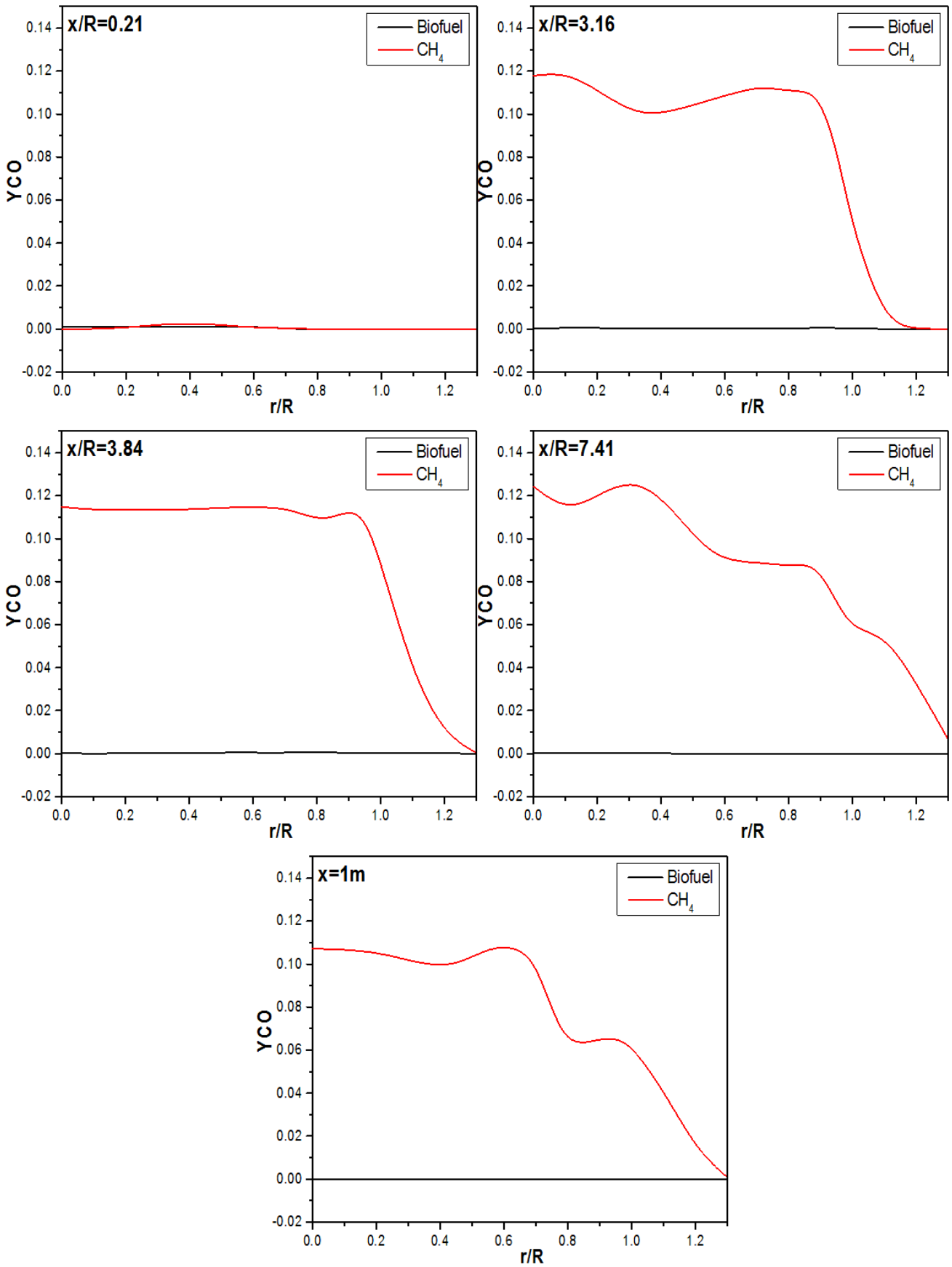

Figures III.9 Comparison of CO mass fraction of CH_4 and Bio fuel.

III.2.2.2 Temperature

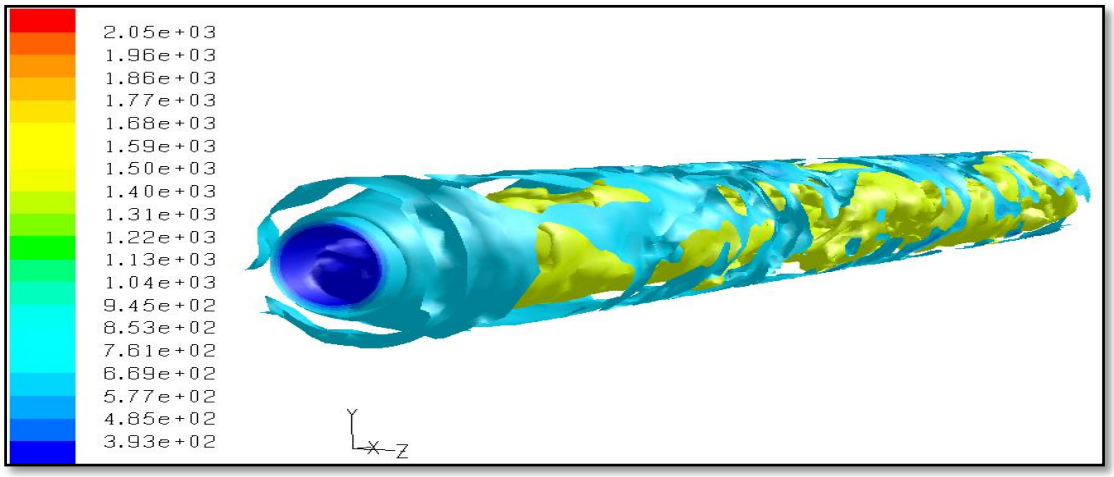

Figure III.10 Temperature (K) distribution in the burner of Biofuel/Air combustion(3D).

The figures III.11 represent the difference between the Bio fuel and the CH4 temperatures distributions in the combustion chamber. We can see that the profiles have the same tendency for both combustibles with the difference of 15%. In the flame zone the temperature profiles present a peak (1600K), and then decrease to equal the walls temperature (500K). The high values of temperature are situated in the flame, because this zone is the same zone of chemical reactions, and these reactions are considered as exothermic reactions. The temperature values decrease when we get away to the flame zone. The difference in the temperature of the Bio fuel and the CH_4 can be interpreted by the difference in the adiabatic temperature that characteristic each flue.

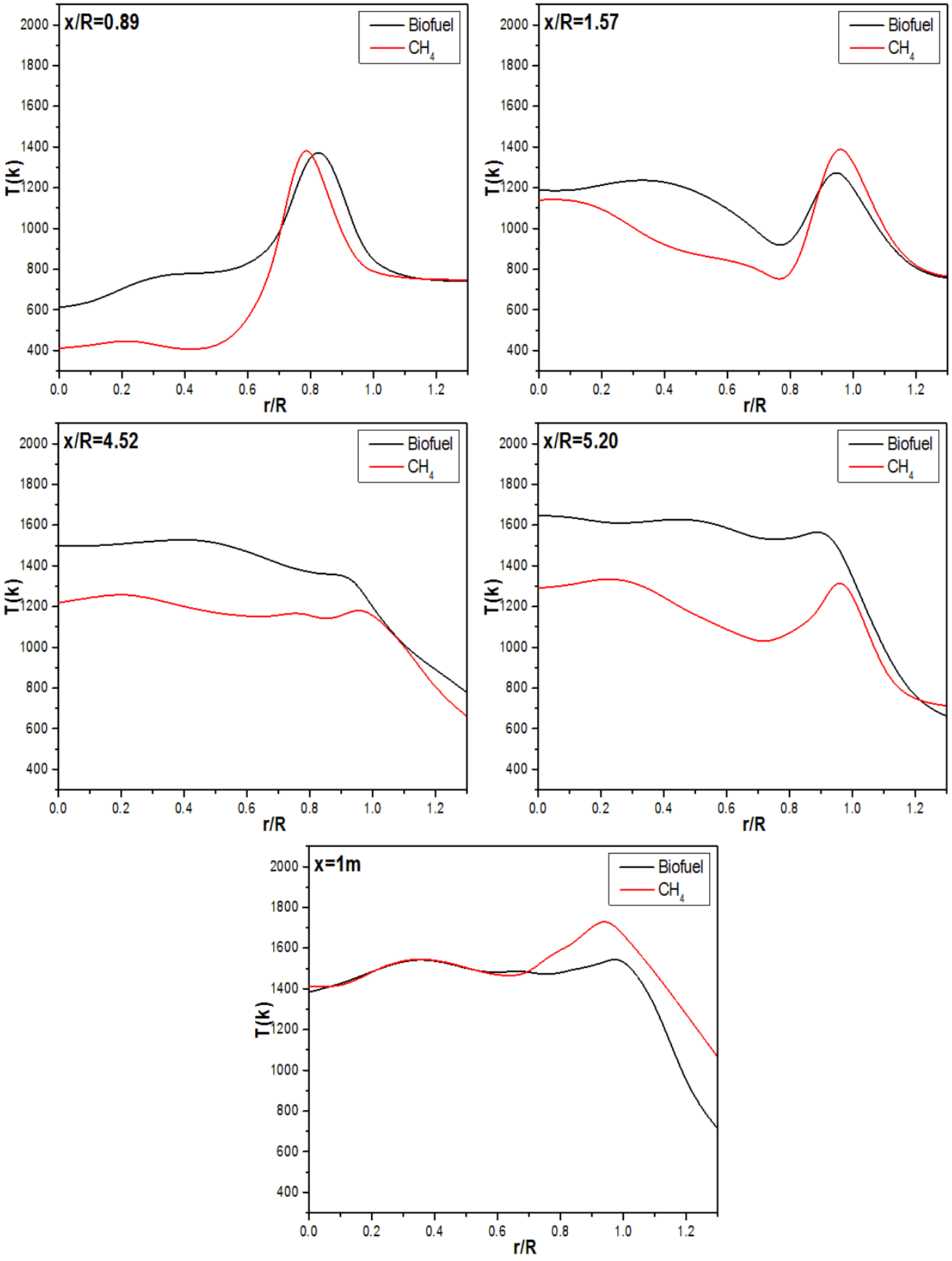

Figures III.11 Comparison of Temperature of CH_4 and Bio fuel.

III.2.3.3 Axial velocity

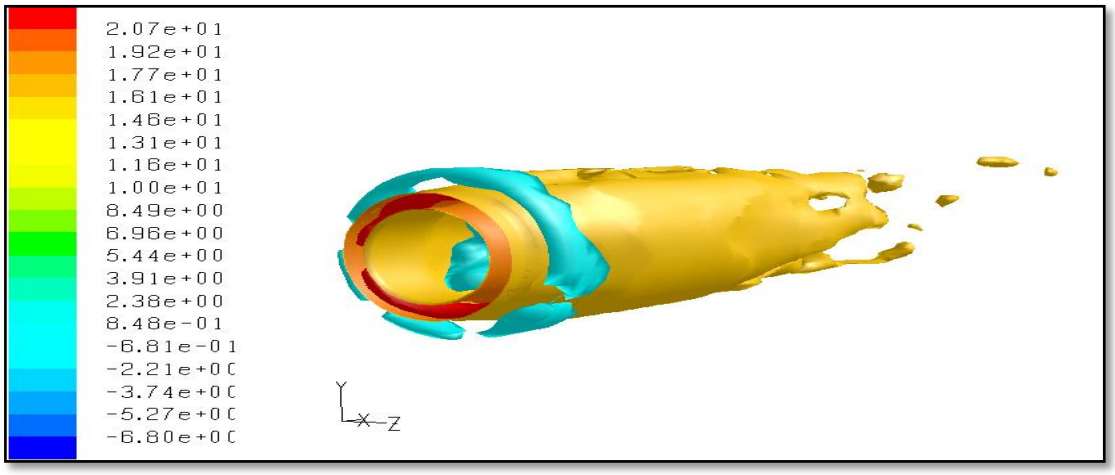

Figure III.12 Velocity (m/s) distribution in the burner of Biofuel/Air combustion (3D).

The figures III.13 illustrate the comparison between the velocity of the Bio fuel and CH_4 in different stations inside the combustion chamber. We can observe that the profiles of the two combustibles have the same tendency, where the difference between the two profiles is given by 57.3%. The high values in the graphs presented by the peak; where it is located in the flame zone. In this zone, the velocity ratio values are greater than 1. We can also see negative values in the velocity profiles that show the recirculating regions: in the center of the burner and near the walls. These zones are vanished when we get away to the inlet of the combustion chamber (see the fourth and the fifth stations). We observe that the velocity of the methane is greater than the velocity of the Bio fuel caused by the mass of the methane lower than Bio fuel mass.

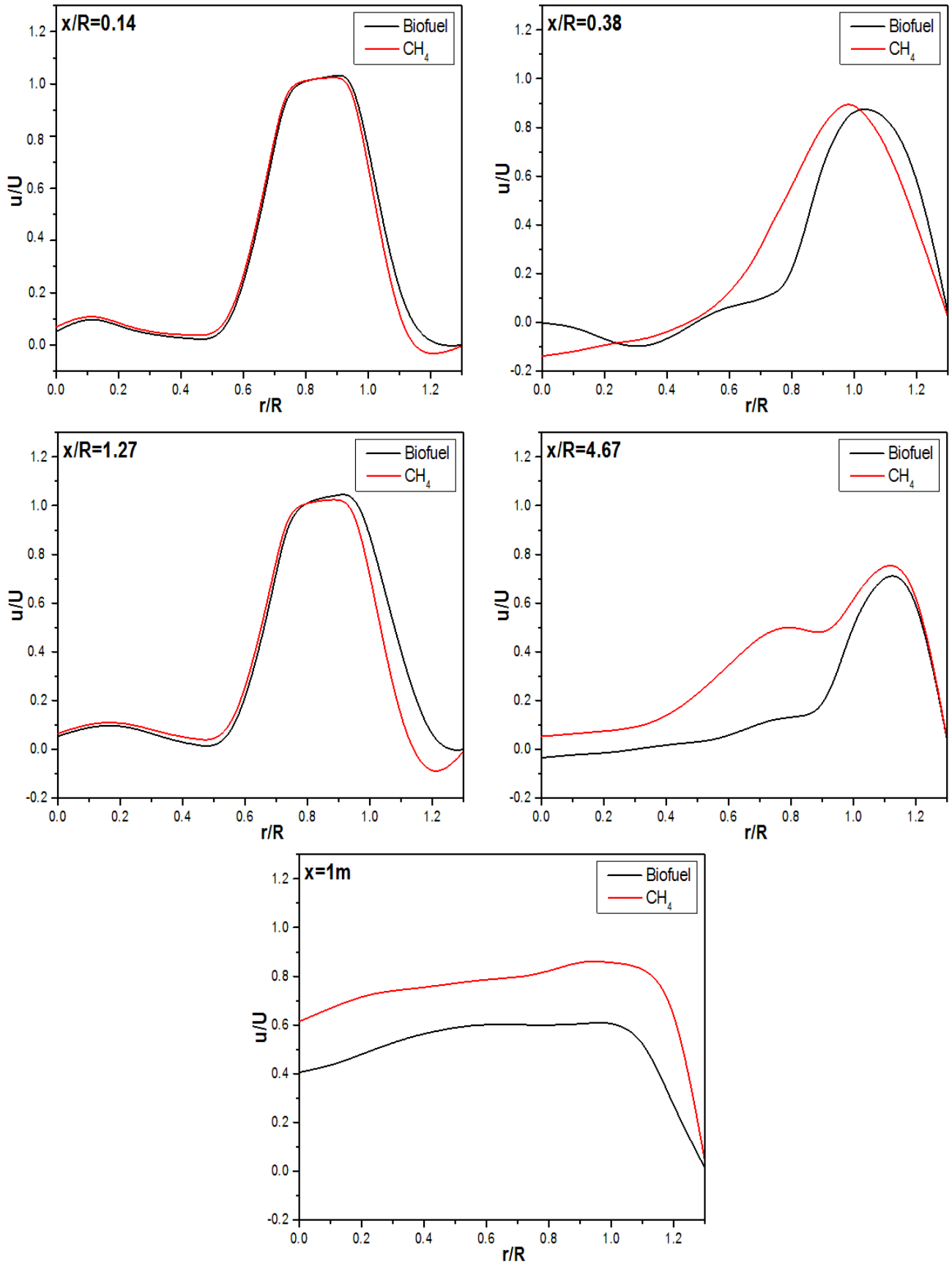

Figures III.13 Comparison of X-Velocity in CH_4 and Bio fuel.

Conclusion

In this chapter, we exposed and explained the results obtained by the numerical simulation using CFD-FLUENT tools in turbulent non premixed combustion fueled by biofuel/air. Also, we investigated numerically with the LES-WALE model coupled with the Beta-PDF approach in the 3D combustion chamber. Moreover, the obtained results are compared with experimental references results. Overall, the simulation results are in acceptable agreement with the experimental reference data. The use of the Bio fuel has an impact on the reduction of the CO in the combustion.

General Conclusion

General Conclusion

Using Bio fuels made from corn, sugar cane and soy could have a greater environmental impact than burning fossil fuels, according to experts. Although the fuels themselves emit fewer greenhouse gases, they all have higher costs in terms of biodiversity loss and destruction of farmland. The problems of climate change and the rising cost of oil have led to a race to develop environmentally-friendly Bio fuels, such as palm oil or ethanol derived from corn and sugar cane. The European Union has proposed that 10% of all fuel used in transport should come from Bio fuels by 2020 and the emerging global market is expected to be worth billions of dollars a year. But the new fuels have attracted controversy. "Regardless of how effective sugar cane is for producing ethanol, its benefits quickly diminish if carbon-rich tropical forests are being razed to make the sugar cane fields, thereby causing vast greenhouse-gas emission increases," Jörn Scharlemann and William Laurance, of the Smithsonian Tropical Research Institute in Panama, write in Science today.

The present work recapitulates the validation of the coupled models (LES/PDF) and the prevision of the Bio fuel behavior flame and the comparison of the methane and the Bio fuel combustion, considered the different stations in the cylindrical combustion chamber, using the FLUENT-CFD package to carry out the computation. The conclusions arising from this investigation as follows:

- The computational results of the coupled dynamic model, LES, and scalar model, PDF, give satisfactory agreement with the experiment data;
- The important role of the shear layers caused by velocity ratio between the fuel and the air to established the flame in the burner;
- The flame seated on the shear layers because it is the mixture region more rich;
- The high velocity values located around the flame holder;

- The production of CO are well predicted by the present computation as the probability density function model uses multi species to approach the reality reaction mechanism,
- The relation between the temperature and the carbon monoxide is proportional. Or, the temperature decrease when the hydrogen increase in the reactive mixture,
- The Bio fuel reduces the pollutants in the combustion produce species like as the emission of CO.
- The Bio fuel is considered as a clean fuel comparatively to the methane.

Furthermore, this study can be extended by the using of the second law of thermodynamic to predict the different sources of the entropy generation (friction, heat and chemical); in order to select the case with optimized energy for the appropriate fuel (methane or Bio fuel).

References

[1] W.C.WANG, L.TAO, "*Bio-jet fuel conversion technologies*", Renewable and Sustainable Energy Reviews 53 801-822 (2016).

[2] J.R.KERIENÈ, *et al*, "*Action of the Products of Bio fuel Combustion on the Phase Composition and Structure of Refractory Material*", Glass and Ceramics Vol 72, pp 345-350(2016).

[3] L.ZHOU, *et al*, "*Numerical study of influence of biofuels on the combustion characteristics and performance of aircraft engine system*", Applied Thermal Engineering 91 399-407 (2015).

[4] F.E.M.ALAOUI, *et al*, "*Excess enthalpies of ternary mixtures of (oxygenated additives + aromatic hydrocarbon) mixtures in fuels and bio-fuels:(Dibutyl-ether + 1-propanol + benzene), or toluene, at T = (298.15 and 313.15) K*", J. Chem. Thermodynamics 85 26-34 (2015).

[5] G.GONCA, *"Investigation of the influences of steam injection on the equilibrium combustion products and thermodynamic properties of bio fuels (biodiesels and alcohols)*", Fuel 144 244-258 (2015).

[6] D.C.RAKOPOULOS, *et al*, "*Influence of properties of various common bio-fuels on the combustion and emission characteristics of high-speed DI (direct injection) diesel engine: Vegetable oil, bio-diesel, ethanol, n-butanol, diethyl ether*", Energy 73 354-366 (2014).

[7] M.C.CAMERETTI, *et al*, "*Study of an exhaust gas recirculation equipped micro gas turbine supplied with bio-fuels*", Applied Thermal Engineering 59,162-173 (2013).

[8] S.BRYNOLF, *et al*, "*Environmental assessment of marine fuels: liquefied natural gas, liquefied biogas, methanol and bio-methanol*", Journal of Cleaner Production 74 86-95 (2014).

[9] I.G.PEARMAN, "*Limits to the potential of bio-fuels and bio-sequestration of carbon*", Policy 59 523–535 (2013).

[10] S.MORALES, *et al*, "*Solar biomass pyrolysis for the production of bio-fuels and chemical commodities*", Journal of Analytical and Applied Pyrolysis 109,65-78(2014).

[11] J.HAN, *et al*, "*Life-cycle analysis of bio-based aviation fuels*", Bioresource Technology 105, 447-456 (2013).

[12] F.AGUILAR, *et al*, "*Excess enthalpies of ternary mixtures of oxygenated additives + hydrocarbon mixtures in fuels and bio-fuels: Dibutyl ether (DBE) and 1-butanol and 1-hexene or cyclohexane or 2,2,4 trimethylpentane at 298.15 K and 313.15 K*", J. Chem. Thermodynamics 56 6-11 (2013).

[13] F.BOURAS, F.KHALDI, "*Computational modeling of thermodynamic irreversibilities in turbulent non-premixed combustion*", Heat and Mass Transfer 51 751-900, (2015).

[14] W.K.GEORGE, "*Lectures in Turbulence for the 21st Century*", Department of Aeronautics Imperial College of London, UK (2013).

[15] N.PETERS, "*Turbulent combustion*", Cambridge University Press, UK (2000).

[16] J.SODJA, "*Turbulence models in CFD*", University of Ljubljana Faculty for mathematics and physics Department of physics, Slovenia (2007).

[17] G.FALKOVICH, *et al,* "*Particles and Fields in Fluid Turbulence*", Rev. Mod. Phys. 73, 913 – Published 19 November (2001).

[18] B.I.CELIK, "*Introductory Turbulence Modeling*", West Virginia University Mechanical & Aerospace Engineering Dept, USA (1999).

[19] J.M.DONOUGH, "*Introductory Lectures on Turbulence Physics, Mathematics and Modeling*", Departments of Mechanical Engineering and Mathematics University of Kentucky, USA (2007).

[20] T.ILIESCU, "*Large Eddy Simulation for Turbulent Flows*", Doctoral thesis, University of Pittsburgh, The U.S state of Pennsylvania,1-18 (2000).

[21] M.LESIEUR, *et al,* "*Large-Eddy Simulations of Turbulence*", Cambridge University Press,, USA (2005).

[22] H.XUE, *et al*, "*Comparison of different combustion models in enclosure fire simulation*", Singapore (2000).

[23] L.SEAT, "*Large eddy simulation of flame/acoustic interactions in a spin flow*", Doctoral thesis, University of Toulouse, France (2004).

[24] J.COUSTEIX, "*turbulence and boundary layer*", Cepadues Toulouse, France (1989).

[25] D.RAZAFINDRALANDY, "*Contribution to the mathematical and numerical study of large eddy simulation*", Doctoral thesis, University of La Rochelle, France (2005).

[26] R.M.S.ROSA, "*Turbulence Theories*", Universidade Federal do Rio de Janeiro, Encyclopedia of Mathematical Physics, Brazil (2006).

[27] D.C.WILCOX, "*Turbulence Modeling for CFD*", Third edition copyright © 2006 by DCW Industries, Inc., November, Canada (2006).

[28] S.K.SADASIVUNI, "*LES modelling of non-premixed and partially premixed turbulent flames*", Doctoral Thesis, Loughborough University Institutional Repository, UK (2009).

[29] H.PITSCH, "*Large-Eddy Simulation of Turbulent Combustion*", Annu. Rev. Fluid. Mech. California 38:453–82 (2006).

[30] L.DUCHAMP et H.PITSCH, "*Progress in large-eddy simulation of premixed and partially-premixed turbulent combustion*", Center for Turbulence Research, Annual Research Briefs (2001).

[31] J.SHINJO, *et al,* "Study on flame dynamics with secondary fuel injection control by large eddy simulation", Combustion and Flame,150, 277–291 (2007).

[32] L.SELLE, *et al*, "*Large-eddy simulation of turbulent combustion for gas turbines with reducedchemistry*", Proceedings of the Summer Program (2002).

[33] C.D.PIERCE, P.MOIN, "*Progress-variable approach for large-eddy simulation of non-premixed turbulent combustion*", Journal of Fluid Mechanics 504, pp.73-97 (2004).

[34] P.D.NGUYEN, P.BRUEL, "*Turbulent reacting flow in a dump combustor : experimental determination of the influence of an inlet equivalence ratio difference on the contribution of the coherent and stochastic motions to the velocity field dynamics*", AIAA - 41st Aerospace Sciences Meeting and Exhibit, Reno, USA(2003).

[35] P.D.NGUYEN, "*Experimental Contribution to The study of Unsteady Characteristics of Reagents Stabilized Premixed Turbulent Flows Downstream of a Symmetric Sudden Expansion*", Poitiers, France (2002).

[36] L.WANG, "*Detailed Chemistry, Soot, and Radiation Calculations in Turbulent Reacting flows*", Doctoral Thesis, University of Pennsylvania, USA (2004).

[37] E.LÉVÊQUE, *et al*, "*Shear-improved Smagorinsky model for large-eddy simulation of wall-bounded turbulent flows*", J. Fluid Mech 570 pp.491-502 (2007).

[38] S.C.KO, H.J.SUNG, "*Large-scale turbulent vortical structures inside a sudden expansion cylinder chamber*", Flow, Turbulence and Combustion 68 269–287 (2002).

[39] A.MAMERI, "*Numerical Study of Turbulent Combustion of Lean PremixedMethane/Air Enriched with Hydrogen*", Doctoral Thesis, University of ORLEANS, France (2009).

[40] F.JAEGLE, "*Large eddy simulation of evaporating sprays in complex geometries using Eulerian and Lagrangian methods*", Doctoral Thesis, Institut National Polytechnique de Toulouse – INPT, France (2009).

[41] F.NICOUD, F.DUCROS, "*Subgrid-scale stress modelling based on the square of the velocity gradient tensor*", CERFACS, France (1999)

[42] G.S.CARDELL, "*Flow Past a Circular Cylinder with a Permeable Wake Splitter Plate*", Ph.D Thesis, GALCIT, California (1993).

[43] H.TOUAHRIA, "*Numerical Study of Turbulent Combustion Structures Inside a Cylinder Burner*", These of Master, University of El-oued, Algérie (2013).

[44] F.BOURAS, "*Study of turbulent combustion via probability density functions*", Doctoral thesis, University of HL-BATNA, Algeria 17-37 (2011).

[45] S.R.GUBBA, "*Development of a Dynamic LES Model for Premixed Turbulent Flames*", Doctoral Thesis, Wolfson School of Mechanical and Manufacturig Engineering Loughborough Uiversity, USA (2009).

[46] B.BIRNIR, "*The Kolmogorov-Obukhov Statistical Theory of Turbulence*", Center for Complex and Nonlinear Science and Department of Mathematics University of California (2012).

[47] M.L.HACK, "*Joint Probability Density Function (PDF) Closure of Turbulent Premixed Flames*", dissertation for the degree of Doctor of Sciences, ETH ZURICH, Switzerland (2011).

[48] R.R.CAO, S.B.POPE, "*The Influence of Chemical Mechanisms on PDF Calculations of Non-premixed Piloted Jet flames*", Combustion and Flame 143, 450–470 (2005).

[49] S.B.POPE, "*Combustion modeling using Probability Density Function method*", Institute of Aeronautics and Astronautics, USA, 349-361 (1990).

[50] S.B.POPE, "*The application of PDF Transport Equations to Turbulent Reactive Flows*", Institute of Technology, USA, 1-14 (1982).

[51] W.P.JONES, *et al*, "*Large Eddy Simulation of Hydrogen Auto-ignition with a Probability Density Function Method*", Proceed Jings of the Combustion Institute, 31, 1765–1771 (2007).

[52] B.E.LAUNDER, N.D.SANDHAM, "*Closure Strategies for Turbulent and Transitional Flows*", Cambridge University Press, Austratia (2002).

[53] R.BOURGHI, M.CHAMPION, "*Modélisation et Théorie des Flammes*", Techip-Paris, France (2000).

[54] H.PITSCH, S.FEDOTOV, "*Investigation of scalar dissipation rate fluctuations in nonpremixed turbulent combustion using a stochastic approach*", UK (2000).

[55] C.D.PIERCE, "*Progress-variable approach for large-eddy simulation of turbulent combustion*", PhD thesis, Stanford university, USA (2001).

[56] N.SHELIL, "*Flashback Studies with Premixed Swirl Combustion*", A Thesis Submitted to Cardiff University for the Degree of Doctor of Philosophy in Mechanical Engineering, Institute of Energy Cardiff School of Engineering Cardiff University Cardiff/ UK (2009).

[57] R.KULKARNI, W.POLIFKE, "*Large Eddy Simulation of Autoignition in a Turbulent Hydrogen Jet Flame Using a Progress Variable Approach*", Journal of Combustion,, Article ID 780370, 11 pages, Germany (2012).

[58] O.P.ILIEV, *et al*, "*Recent Advances in Numerical Methods and Applications II*", World Scientific, UK (1999).

[59] L.SELLE, "*Simulation aux Grandes Echelles des Interactions Flamme/Acoustique dans Un écoulement vrille"*, Thèse de Doctorat, Université de Toulouse, France (2004).

[60] K.K.KUO, R.ACHARYA, "*Fundamentals of Turbulent and Multi-Phase Combustion*", John Wiley & Sons, Inc, Canada (2012).

[61] A.C KADAK, T.ZHAI, "*Air Ingress Benchmarking with Computational Fluid Dynamics Analysis*", 2nd International Topical Meeting on High Temperature Reactor Technology, China (2004).

[62] DM.Hargreaves, *et al*, "*The Computational Fluid Dynamics modelling of the autorotation of square, flat plates*", Fluids and Structures 46, 111-133 (2014).

[63] *S.NESIC*, "*Using Computational Fluid Dynamics in Combating Erosion-Corrosion*", Chemical Engineering Science Journal, 61 4086–4097 (2006).

[64] *K.LONG*, "*last Simulation with Shock Tube Testing and Computational Fluid Dynamics Analysis*", ProQuest, USA (2008).

[65] B.R.MUNSON, *et al*, "*Fluid Mechanics*", 7th Edition, John Wiley and Sons (2013).

[66] *T.G*LATZEL, *et al*, "*Computational fluid dynamics (CFD) software tools for micro-fluidic applications A case study*", Computers & Fluids 37 218–235 (2008).

[67] M.TKACZY, "*Flows modeling in automotive engineering*", Copyright by Wrocław University of Technology, Poland (2011).

[68] M.R.CUMMINGS, *et al*, "*Applied Computational Aerodynamics*", Cambridge University Press, UK (2015).

[69] F.BOURAS, *et al*, "*Improvements of the Combustion Characteristics by the Hydrogen Enrichment*", CEIT 2015 Conference Publications, Algeria (2015).

[70] E.Hu, *et al*, "*Experimental and numerical study on lean premixed methane–hydrogen–air flames at elevated pressures and temperatures*", International journal of hydrogen energy, 34 6951-6960 (2009).

[71] F.BOURAS, *et al*, "*Beta-pdf approach for large-eddy simulation of non-premixed turbulent combustion*", International Review of Mechanical Engineering, 4, 358-363 (2010).

[72] F.BOURAS, *et al*, "*Large Eddy Simulation for Lean Premixed Combustion*", The Canadian journal of chemical engineering, Pages 231–237 (2012).

Abstract

In this work, we investigate a numerical study of non-premixed turbulent combustion of Biofuel/Air in a cylindrical 3D combustion chamber using the FLUENT-CFD software package. The closure in the governing equations of turbulent combustion needs to investigate the additional models to surmount this closure. In this study, the combustion modeling is based on the coupled models LES/ PDF. Where, LES describes the turbulence using statistical methods for the velocity components. And the PDF approach is applied to solve the closure problem in the thermo-chemical equations terms of the turbulent combustion. Thereof, the PDF approach introduces of mixture fraction and progress variable as variables to reduce the number of equations and variables. Finally, the obtained results showed a good agreement with the experimental data. Also, it is confirmed that biofuel is a clean fuel.

Keywords: Non-premixed combustion, Turbulence, Bio fuel, LES/ PDF models, CFD.

Résumé

Dans ce travail, nous avons étudié numériquement de la combustion turbulente non prémélangée de biocarburant / air dans une chambre de combustion 3D cylindrique en utilisant le logiciel FLUENT-CFD. La fermeture dans les équations de combustion turbulente nécessite d'introduire des modèles supplémentaires pour surmonter cette fermeture. Dans cette étude, la modélisation de la combustion est basée sur le couplage des modèles LES / PDF. Où, LES utilise des méthodes statistiques pour les composantes de la vitesse le l'écoulent turbulent. L'approche PDF est appliquée pour résoudre le problème de fermeture dans les termes des équations thermochimiques de la combustion turbulente. L'approche PDF considère la fraction de mélange et le variable de progression en tant que des variables afin de réduire le nombre des équations et des variables. Les résultats obtenus montrent un bon accord avec les données expérimentales. En outre, on a confirmé que le biocarburant est un combustible propre.

Mots clés: Combustion non-prémélangée, Turbulence, Biocarburant, modèles LES/PDF, CFD.

الملخص

في هذا العمل قمنا بدراسة عددية لإحتراق مضطرب غير ممزوج لـ وقود حيوي/هواء في غرفة إحتراق إسطوانية ثلاثية الأبعاد بإستخدام برنامج FLUENT-CFD. لكن مشكلة إنغلاق المعادلات التي تصف الاحتراق المضطرب تحتاج إلى نماذج إضافية لرفع هذا الإنغلاق. في هذه الدراسة نَمذَجة الاحتراق إعتمدت على الازدواج LES/PDF. حيث أُستخدم نموذج LES لوصف الإضطراب بطرق إحصائية بالنسبة لمركبات السرعة. بينما نموذج PDF طبق لحل مشكلة إنغلاق الحدود الحرارية و الكيميائية في معادلات الاحتراق المضطرب، حيث أن هذا النموذج يدخل كل من متغير التقدم و كسر الخليط كمتغيرين للحد من عدد المعادلات و المتغيرات. و في النهاية النتائج التي تم الوصول إليها أعطت توافق جيد مع البيانات التجريبية، كما أكدت على أن الوقود الحيوي هو وقود نظيف.

الكلمات المفتاحية: احتراق غير ممزوج، الاضطراب، وقود حيوي، نموذجي LES/PDF، CFD.